

POLYNOMIAL HISTOPOLATION, SUPERCONVERGENT DEGREES OF FREEDOM, AND PSEUDOSPECTRAL DISCRETE HODGE OPERATORS

N. ROBIDOUX*

Abstract. We show that, given a histogram with n bins—possibly non-contiguous or consisting of single points—there exists a unique polynomial histopolant (polynomial of order n with bin averages equal to the histogram’s). We also present histopolating cardinal functions for histograms with contiguous bins.

The Hodge star operator from the theory of differential forms is the mapping which puts k - and $(d - k)$ -forms on a d -manifold into one-to-one correspondence. For $k = d$, the star operator is a bijective mapping between d -forms (“densities”) and 0-forms (“scalar functions”); a discrete analog is an operator which, given the integrals of a function over n cells, reconstructs (approximately) the values of the function at n nodes. We use histopolants to construct discrete Hodge star operators based on univariate polynomials.

More generally, consider a linear operator which converts n degrees of freedom associated with univariate functions—integrals, averages and/or point values of a function and its derivatives, expansion coefficients with respect to polynomials bases, etc.—to n nodal values. Suppose that this operator is exact on \mathbb{P}_n , the space of polynomials of order n . Is it possible to choose the nodes so that the operator is actually exact on \mathbb{P}_{n+1} ? We characterize the operators for which this is possible, and show that the “optimal” nodes are unique if they exist. We then give explicit formulas for the optimal nodes which correspond to star operators based on histopulation. For example, discrete Hodge star operators based on dual Legendre grids are superconvergent.

Numerical tests confirm the superconvergence and show that the matrix representations of discrete star operators are close to the identity when dual Legendre or Chebyshev grids are used.

Key words. Discrete Hodge star operator, area matching property, polynomial histopulation, inter-histopulation, conversion between nodal values and other degrees of freedom, superconvergence.

AMS subject classifications. 65D05, 65D32, 41A10, 41A25, 74S25

1. Introduction. This article is organized around three related topics: 1D polynomial histopulation, discrete Hodge star operators, and superconvergent linear operators which convert arbitrary degrees of freedom to point values.

1.1. Polynomial smoothing of gappy histograms, and “histograms” with bins consisting of single points. The word “histogram” is used quite loosely in this article: The heights and widths of the bars may be arbitrary real numbers, and the bins—the “bases” of the bars, also called cells in this article—may not be contiguous. That is, there may be gaps between bars, in which case we say that the histogram is gappy.

Given a histogram, a *histopolant* is a continuous function whose cell averages are the same as the histogram’s [18, 21, 43, 44, 46]. It is easy to show that every histogram based on n contiguous bins can be histopolated with a polynomial of order n (key idea: one antiderivative of the histopolant interpolates the histogram’s cumulative integral at bin endpoints) [12, 30, 45]. We extend this result to gappy histograms, and to “*histograms*” with bins consisting of single values, for which the average matching property boils down to interpolation. Specifically, we prove that there exists a unique polynomial of order n which interpolates m point values and histopolates $n - m$

*Department of Mathematics, Simon Fraser University, Burnaby BC V5A 1S6, Canada. Email: nrobidou@pims.math.ca. Research funded by Natural Sciences and Engineering Research Council of Canada (NSERC) grants OGP000871 and OGP0036901. The hospitality of the Pacific Institute for the Mathematical Sciences at Simon Fraser University was appreciated.

averages, provided the averages are computed over intervals with disjoint interiors and the points are distinct and located anywhere but in the interiors of the intervals.

1.2. Discrete Hodge star operators. Discrete Hodge star operators and discrete constitutive relations perform conversions between point values and cell averages, between edge circulations and total face fluxes, etc. Such conversion operators have been identified as important components of mixed finite element, finite volume and finite difference methods for the numerical solution of partial differential equations [2, 6, 7, 8, 22, 27, 28, 31, 32, 33, 39, 41, 47, 49, 51, 52].

1.2.1. An important simplification: identifying differential forms with functional proxies. There is a close relationship between the material presented in this article and models of continuum mechanics based on cochains, coboundary operators, discrete constitutive relations and Tonti diagrams [5, 13, 14, 15, 19, 20, 35, 36, 37, 38, 53, 54, 56]. However, no deRham cohomology or differential forms theory is needed to understand this article. Because we identify discrete differential forms with polynomial proxies, and we restrict ourselves to trivial material properties and constitutive relations, (continuum) Hodge star operators “look” like identity mappings, and discrete Hodge star operators can be defined in an elementary way [39].

1.2.2. Discrete Hodge star operators: nodal values to cell masses. Given the values of some real function f at n distinct nodes in \mathbb{R}^d , an estimate for the integral of f over a measurable set C may be obtained by interpolating the nodal values and integrating the interpolant over C , that is, with an interpolatory quadrature or cubature rule [17, 24]. The simultaneous approximation of the integrals of f over n distinct measurable sets is of particular interest: the corresponding mapping, from n nodal values to n integrals, is a discrete analog of the Hodge star operator of differential forms theory which maps 0-forms to d -forms.

1.2.3. Discrete Hodge star operators: cell masses to nodal values. Conversely, given the values of the integrals of a real function f over n suitable measurable subsets C_i of \mathbb{R}^d , an estimate for the value of f at a node may be obtained by constructing a function which is consistent with this data, and evaluating this function at the node (by analytic substitution). If $d = 1$ and the C_i ’s are bounded intervals with disjoint, nonempty interiors, this corresponds to evaluating a histopolant. Of particular interest is the simultaneous approximation of the values of f at n distinct nodes, a discrete analog of the Hodge star operator which maps d -forms to 0-forms.

For a given space of differential forms proxies (polynomials, trigonometric polynomials, splines, radial basis functions, etc.), the discrete Hodge star operator which maps cell masses to nodal values is the inverse of the discrete Hodge star operator which maps nodal values to cell masses.

1.2.4. 1D discrete Hodge star operators consistent with boundary conditions. In this article, we study discrete Hodge star operators on the interval ($d = 1$). Hybrid discrete Hodge star operators which map $n - 1$ cell integrals and one boundary point value, or n point values to $n - 2$ cell integrals and two boundary point values, to n nodal values, arise when solving two point boundary value problems. Following is a list of the discrete Hodge star operators which are most relevant:

- discrete Hodge star operators which converts n integrals to n interior point values;
- discrete Hodge star operators which converts $n - 1$ integrals and one boundary value to $n - 1$ interior point values and one boundary value (at the same boundary point);

- discrete Hodge star operators which converts $n - 2$ integrals and two boundary values to $n - 2$ interior point values and two boundary values; and
- discrete Hodge operators which converts n integrals to $n - 2$ interior point values and two boundary values.

The above four discrete Hodge star operators and their inverses, together with variants which map averages instead of integrals, are discussed in detail in this article.

1.3. Cell masses VS cell averages. Histopolation is usually defined by way of matching bin integrals (bar areas), not bin averages (bar heights). When the bins are intervals with positive lengths, matching averages is equivalent to matching areas. When some or all of the bins are singletons, however, the corresponding bars have vanishing areas regardless of their heights. In this situation, it is natural to define the “average” of a function over a singleton $\{x\}$ to be $f(x)$. With this definition, matching “averages” generalizes both histopolation and interpolation.

Integrals have the additional disadvantage of not scaling like point values. In contrast, averages are $\mathbf{O}(1)$ quantities irrespective of grid spacing. We often present results in terms of rescaled discrete Hodge star operators which map cell averages to point values. Because nodal values approximate cell averages when nodes are close to the cells—this is actually a second order approximation when the nodes are located at cell centers—the matrix representations of discrete Hodge star operators which map averages to point values are close to the identity matrix.

1.4. Dual grids. Two grids are used when constructing discrete Hodge star operators: a (primal) grid which defines the cells, and a (dual) grid which defines the nodes. Given one of the two grids, one would like to know how best to generate the second so that truncation error be minimized. We will see that it is preferable to optimize the nodal grid given the cell grid.

1.5. Superconvergent conversion between arbitrary degrees of freedom and nodal values. Discrete Hodge star operators convert values associated with one projection—say, point values—to values associated with another—say, cell masses.

We prove a general theorem about operators which convert n nodal (point) values to n “other” degrees of freedom (point values of the function or its derivatives, cell masses or averages, expansion coefficients with respect to a polynomial basis, etc.) by way of polynomial proxies. By construction, such operators are exact on \mathbb{P}_n ; likewise for their inverses. The theorem asserts that the conversion operator and its inverse are exact on \mathbb{P}_{n+1} —a gain of one order—if and only if the nodes are the roots of a polynomial of degree n which depends solely on the alternate degrees of freedom. We call such roots “optimal nodes.”

Optimal nodes always exist when the alternate degrees of freedom are combinations of point values, masses and/or averages (provided the intervals over which integrals or averages are computed have disjoint interiors and the points are distinct and are located anywhere but in the interiors of the intervals). Consequently, it is possible to make the corresponding discrete star operators exact on polynomials of order $n + 1$, a form of superconvergence. For example, the discrete Hodge star operator which converts n integrals to n interior point values is exact on \mathbb{P}_{n+1} if the cells extend between ± 1 and the extrema of the Legendre polynomial P_n , and the nodes are located at the roots of P_n .

1.6. Piecewise polynomial bases. We only use global polynomial bases in this article. However, the results are easily adapted to piecewise polynomial bases. In particular, we believe that geometric degrees of freedom for higher order conformal

finite elements in $\mathbb{H}(\text{div})$ and $\mathbb{H}(\text{grad})$ should be located so that the corresponding dual grids be optimal [3, 4, 10, 11, 25, 29].

2. Outline. In Section 4, we establish the existence and uniqueness of histopolants for histograms with or without gaps (Theorem 4.1).

In Section 5, we give formulas for the cardinal basis polynomials which correspond to histograms with contiguous bars.

In Section 6, having defined inter-histopolants—inter-histopolants are polynomials with prescribed point values *and* cell averages—we proceed to establish their existence and uniqueness (Theorem 6.5). When there are no gaps, the inter-histopolant is equal to the derivative of an easily constructed Hermite interpolant (Theorem 6.7).

In Section 7, we define generic star operators and prove their elementary properties. Star operators are linear operators which convert arbitrary degrees of freedom to nodal values, by way of polynomial proxies. A number of examples are discussed: discrete Hodge star operators, mappings which convert spectral coefficients to point values, mappings which map weighted integrals over intervals with distinct interiors to point values, etc.

In Section 8, we define (formal) superconvergence: A linear operator which maps n degrees of freedom to n nodal values is superconvergent if it is exact on polynomials of order $n + 1$. We then prove the central result of the paper: A linear operator which maps n degrees of freedom to n nodal values is superconvergent if and only if the nodal degrees of freedom are defined by the roots of a polynomial for which the alternate degrees of freedom vanish. We call such roots “optimal nodes” (Theorem 8.7).

In Section 9, we illustrate the generality of Theorem 8.7 by showing that optimal nodes exist for operators which convert polynomial expansion coefficients to nodal values. The nodes which are optimal for truncated orthogonal polynomial expansions are found to be the roots of the first excluded basis polynomial.

In Section 10, we show that optimal nodes exist for star operators which convert n point values, cell averages and/or integrals, to n nodal values, provided the corresponding inter-histopolant problem is well-defined (Theorem 10.1). We also show that there is an optimal node in every cell, and that the locations of the optimal nodes can be determined without solving an inter-histopolant problem (Theorem 10.2).

In Section 11, we show that the first three discrete Hodge star operators listed above in Section 1.2.4 can be made superconvergent (Corollary 11.1). The fourth discrete Hodge star operator, which converts n integrals to $n - 2$ interior point values and two boundary values, cannot be made superconvergent, because optimal nodes corresponding to integral degrees of freedom must be located in the interiors of the intervals, yet two nodes are located at the boundary.

Legendre polynomials P_n and Chebyshev polynomials T_n are examples of Jacobi polynomials $P_n^{(\alpha, \beta)}$. In Section 12, we establish that the only Jacobi polynomial roots grids which are optimal for extrema and endpoints grids are P_n ($= P_n^{(0,0)}$), $P_n^{(1,0)}$, $P_n^{(0,1)}$ and $P_n^{(1,1)}$ (Theorem 12.3). Note that the extrema and endpoints grids corresponding to other polynomials (for example, Chebyshev polynomials) do define optimal nodes; it is just that in general the optimal nodes are not given by the corresponding roots grids.

In Section 13, we explain why it is preferable to optimize the nodal degrees of freedom. Essentially, this is because the “dual” optimization problem is not well-posed (Theorem 13.3).

The remainder of the article is devoted to a numerical study of the discrete star operators which convert n averages to n nodal values. Discrete Hodge star operators based on Legendre, Chebyshev, and uniform grids yield spectrally accurate nodal values and integrals for sufficiently smooth test functions. (Only algebraic convergence is observed when a discontinuous test function is used, and then, only in RMS norm.) Most importantly, the formal superconvergence is shown to translate into accelerated convergence rates; in the case of the test function e^x , for example, MAX errors with optimized Chebyshev nodes are $\mathbf{O}(1/n^2)$ relative to the MAX errors with nodes located at the Chebyshev roots, and the RMS errors are $\mathbf{O}(1/n)$. Also, the matrix representations of discrete star operators based on Legendre and Chebyshev extrema and endpoints grids have condition numbers bounded by 2 and to be close to the identity matrix. Optimal grids yield matrices which are closer to the identity and have smaller condition numbers.

3. Terminology and notation.

- average:** The average of the function f over the interval C_i is $\frac{1}{h_i} \int_{C_i} f dx$.
- “average:”** The “average” of the function f over the interval C_i is the usual average; the “average” of f over the singleton $\{x_j\}$ is $f(x_j)$. (In this article, quotes often indicate that point values being are used in addition to integrals or averages.) §6.
- bins:** n bounded intervals which define the bases of the bars of a histogram. §1.1, §4.
- cardinal basis function:** Given a set of degrees of freedom, a cardinal basis function is one for which all degrees of freedom but one vanish, the nonzero degree of freedom being equal to 1. For example, Lagrange polynomials are cardinal for point degrees of freedom, because they vanish at all grid points but one, where they take the value 1. §5, §7.1.
- cell:** A bounded nonempty interval or a singleton. The cells define the bins of a “histogram.” §6.2.
- commutative diagram:** A diagram commutes if any two compositions of mappings which start and end at the same place are equal. §7.3.
- C_i : The i th cell (out of n). §6.2.
- degrees of freedom:** n numbers which completely determine a polynomial of order n . §7.
- extrema and endpoints grid:** A grid with points at the endpoints of $[-1, 1]$ together with the extrema of a given polynomial (usually orthogonal). §12.1.
- faces:** The boundary points of the cells (endpoints for intervals, singleton points otherwise). §6.2.
- gappy histogram:** An histogram with gaps (with some bars “missing”). §1.1, §4.
- H:** Diagonal matrix of the cell lengths h_i . §14.4.
- Hermite interpolant:** An interpolating polynomial with prescribed derivatives at some or all of the interpolation abscissa.
- histogram:** n intervals with non-intersecting interiors together with n corresponding averages (bar heights) or, equivalently, integrals (bar areas). Note: There may be gaps between bins, that is, the intervals defining the histogram may not be contiguous. §1.1.
- “histogram:”** n cells together with n corresponding “averages.” §6.
- histopolant:** A continuous function whose bin averages are the same as the histogram’s. §1.1, §4.
- inter-histopolant:** A continuous function whose cell “averages” are the bar heights, that is, a continuous function which interpolates several point values and matches several bar areas. §6.3.
- h_i : The length of the i th cell. §4.
- interval:** (a, b) , $[a, b)$ or $(a, b]$ with $-\infty < a < b < \infty$.
- I:** Identity matrix.
- l_i : Cardinal basis polynomial (Lagrange polynomial) with respect to the faces. §5.
- l_i^* : Cardinal basis polynomial (Lagrange polynomial) with respect to the nodes. §7.1.
- nodes:** Points which define the projection operator π_0^* and the nodal degrees of freedom. §7.1.
- optimal nodes:** For a given π , the unique nodes which make the corresponding \star and its inverse superconvergent. §8.
- optimized grid:** A dual grid for which the discrete star operator and its inverse are superconvergent. §10.
- polynomials of order n :** A polynomial of order n is a polynomial of degree at most $n - 1$.
- φ_i : Cardinal basis polynomial with respect to integral projections. §5.
- $\bar{\varphi}_i$: Cardinal basis polynomial with respect to average projections. §5.
- P_n : Legendre polynomial of degree n .
- $P_n^{(\alpha, \beta)}$: Jacobi (hypergeometric) polynomial of degree n .

\mathbb{P}_n : The space of univariate polynomials of order n (of degree at most $n - 1$).

regular C_i 's: "Sufficiently disjoint" intervals and singletons. §6.2.

roots grid: A grid with points at the roots of a given polynomial. §12.1.

singleton: A set which consists of one point. §6.

superconvergent: Exact on \mathbb{P}_{n+1} even though only n degrees of freedom are used. §8.

T_n : Chebyshev polynomial of the first kind of degree n .

x_i : The i th face (there may be up to $2n$ faces). §5, §10.2.

x_i^* : The i th node (out of n). §7.1.

$\mathbf{0}$: Matrix, or column vector, with vanishing entries.

ι : Inverse of the restriction of π to \mathbb{P}_n . §7.3. For example, the operator which associates to a histogram the corresponding histopolant. §14.3.

π_0^* : Interpolation operator: mapping which reconstructs the unique polynomial of order n which takes n prescribed values at the nodes. §7.1.

π : Linear mapping, from a function space containing \mathbb{P}_{n+1} into \mathbb{R}^n , which is one-to-one on \mathbb{P}_n . π maps smooth functions to n degrees of freedom. §7.3. For example, mapping which associates to a function its integrals over n intervals. §14.2.

$\bar{\pi}$: Mapping which associates to a function the column vector of its averages over n intervals. §14.2.

π_0^* : Mapping which associates to a function the column vector of its point values at the n nodes. §7.1.

ρ : $\rho(q) := q - \iota\pi(q)$. §8.

\star : $\pi_0^*\iota = (\pi_0^*)^{-1}$. §7.3. Also, mapping which associates n point values to n cell integrals and point values. §10.

$\bar{\star}$: Mapping which associates n point values to n cell averages and point values. §14.4.

4. Histopolants for gappy histograms exist and are unique. In this section, we establish the existence and uniqueness of histopolants for histograms with possibly non-contiguous bars. (In Section 6.3, we prove existence and uniqueness in cases in which some the bins are singletons.)

THEOREM 4.1. *Given a histogram defined by n bins C_i —bounded intervals with lengths $h_i > 0$ and disjoint interiors—and corresponding bar heights $f_i \in \mathbb{R}$, there exists a unique histopolant in \mathbb{P}_n , that is, a unique $p \in \mathbb{P}_n$ such that*

$$\frac{1}{h_i} \int_{C_i} p \, dx = f_i, \quad i = 1, \dots, n.$$

(Equivalently, one can match bin integrals.)

Proof. Because \mathbb{P}_n is an n -dimensional vector space and mapping a function to its values at n points is linear, uniqueness implies existence. Consequently, it is sufficient to show that $p \equiv 0$ if $f_i = 0$ for all i . So, suppose that the bin averages of p vanish. Because p is continuous and C_i is an interval with nonempty interior, p must vanish somewhere in the interior of C_i by the Intermediate Value Theorem. The interiors of the bins being disjoint, p must have n distinct (real) roots. The degree of p being less than n , p must be trivial. \square

5. Cardinal basis polynomials for histograms with contiguous bars. The matrix entries of discrete Hodge star operators which map n integrals or averages to n nodal values can be given in closed form in terms of histopolating cardinal basis functions. In this section, we give formulas for histopolating cardinal basis functions which correspond to histograms without gaps.

DEFINITION 5.1. *Suppose that C_i runs from $x_{i-1/2}$ to $x_{i+1/2}$, $i = 1, \dots, n$, where $-\infty < x_{1/2} < \dots < x_{n+1/2} < \infty$ (so that the bins are contiguous). Then, $\ell_{i+1/2}$ is the Lagrange polynomial corresponding to $x_{i+1/2}$, that is, the polynomial of degree n which vanishes at all $x_{k+1/2}$'s except $x_{i+1/2}$, where it takes the value 1.*

$$\ell_{i+1/2} := \prod_{k \neq i} \frac{x - x_{k+1/2}}{x_{i+1/2} - x_{k+1/2}}, \quad i = 0, \dots, n.$$

The Lagrange polynomials are cardinal, that is, $\ell_{i+1/2}(x_{j+1/2}) = \delta_i^j$ [9].

When the bins are contiguous, an antiderivative of a histopolating cardinal basis function must interpolate a step function with a unit jump in the interior of the corresponding bin by the Fundamental Theorem of Calculus [12, 30, 45].

THEOREM 5.2. *Suppose that the bins are contiguous, and let*

$$\wp_j := \sum_{k=j}^n \ell'_{k+1/2} = \frac{1}{2} \sum_{k=j}^n \ell'_{k+1/2} - \frac{1}{2} \sum_{k=1}^j \ell'_{k-1/2}.$$

Then, $\{\wp_i\}_{i=1}^n$ is a cardinal basis with respect to integral projections, that is,

$$\int_{C_i} \wp_j dx = \delta_i^j.$$

Likewise, $\bar{\wp}_j := h_j \wp$, where h_j is the length of C_j , is a cardinal basis polynomial with respect to average projections, that is,

$$\frac{1}{h_j} \int_{C_i} \bar{\wp}_j dx = \delta_i^j.$$

Proof.

$$\sum_{k=j}^n \ell_{k+1/2}(x_{i+1/2}) = \sum_{k=j}^n \delta_k^i = \begin{cases} 0 & \text{if } i < j, \\ 1 & \text{if } i \geq j. \end{cases}$$

Consequently, $\sum_{k=j}^n \ell_{k+1/2}$ interpolates “step-function” data on the $x_{i-1/2}$ ’s, with the unit jump located in the interior of C_j , and

$$\int_{C_i} \wp_j dx = \int_{x_{i-1/2}}^{x_{i+1/2}} \wp_j dx = \sum_{k=j}^n \ell_{k+1/2}(x_{i+1/2}) - \sum_{k=j}^n \ell_{k+1/2}(x_{i-1/2}) = \delta_i^j.$$

($\sum_{k=j}^n \ell'_{k+1/2} = \frac{1}{2} \sum_{k=j}^n \ell'_{k+1/2} - \frac{1}{2} \sum_{k=1}^j \ell'_{k-1/2}$ because $\sum_{k=0}^n \ell_{k+1/2} \equiv 1$.) \square

6. Matching averages and point values. In this section, we extend Theorem 4.1 to “histograms” with bins consisting of single values, for which the average matching property reduces to interpolation. At the end of the section, the construction of “inter-histopolants” is reduced to Hermite interpolation when the bins are contiguous.

6.1. “Averaging” over a singleton. “Interpolation/histopolation” problems can be stated concisely by redefining averaging so it applies to singletons.

DEFINITION 6.1. *The “average” of a function f over the singleton $\{x\}$ is $f(x)$.*

(Note: The “average” of a Lebesgue integrable function over a singleton $\{x\}$ is the limit of averages over intervals which shrink nicely to x [42]. For this reason, “bars” associated with singletons can be understood as limits.)

6.2. Regular families of subsets of the real line. We now define families of subsets of the real line for which unique “inter-histopolants” exist for arbitrary data.

DEFINITION 6.2. *A cell is a bounded nonempty connected subset of \mathbb{R} . Consequently, a cell is either a singleton or a bounded interval with nonempty interior.*

DEFINITION 6.3. *A collection of cells $\{C_i\}$ is regular provided the following conditions hold:*

- *if C_i and C_j have nonempty interiors and $i \neq j$, then C_i and C_j have disjoint interiors,*
- *if C_i and C_j are singletons and $i \neq j$, then C_i and C_j are disjoint, and*
- *if C_i is a singleton and C_j has nonempty interior, then C_i is not contained in the interior of C_j .*

DEFINITION 6.4. *A face is a boundary point of a cell (interval endpoint if the cell has positive length, the singleton point itself otherwise).*

If there are n cells, there are at least n faces (if the cells are singletons) and at most $2n$ faces (if the cells are separated intervals).

Although regularity, as a property, applies to *families* of subsets of the real line, we will often abuse language and say that the subsets themselves are regular.

EXAMPLE 1 (Regular subsets of the real line). *The cells $C_1 = [0, 1]$, $C_2 = \{1\}$, $C_3 = [1, \sqrt{2}]$, $C_4 = \{\sqrt{3}\}$, $C_5 = (\pi, 5)$, $C_6 = (5, 8)$, $C_7 = \{8\}$, $C_8 = \{17/2\}$, $C_9 = [9, 13]$, $C_{10} = [13, 14]$ and $C_{11} = \{16\}$ are regular. The corresponding faces are $0, 1, \sqrt{2}, \sqrt{3}, \pi, 5, 8, 17/2, 9, 13, 14$ and 16 .*

J. H. Verner has observed that the key property of regular families of subsets of the real line is that they can be ordered from “left” to “right” [55]. For example, connectedness is not necessary. The consequences of this observation will be discussed in a separate paper.

6.3. Inter-histopolants exist and are unique. We are now ready for the first main theorem of this article.

THEOREM 6.5. *Given n numbers f_i and n regular cells C_i , there exists a unique $p \in \mathbb{P}_n$ such that the “average” of p over C_i equals f_i for all i .*

Proof. *The proof parallels that of Theorem 4.1. Suppose that the “averages” of $p \in \mathbb{P}_n$ over the cells vanish. Then, every C_i which is not a singleton must have a root of p in its interior. Furthermore, because “averages” correspond to point values for singletons, p must also vanish at singleton points. Because the cells are regular, p must have n distinct roots. \square*

DEFINITION 6.6. *The polynomial p of Theorem 6.5 is called an inter-histopolant.*

Theorem 6.5 bridges interpolation and histopolation: When all cells are singletons, it states the existence and uniqueness of an interpolant; when all cells have positive lengths, the existence and uniqueness of an histopolant; and, when some of the cells are singletons and some have positive lengths, the existence and uniqueness of an inter-histopolant.

6.4. Construction of the inter-histopolant when the cells are contiguous. In this section we show that the construction of an inter-histopolant can be reduced to the evaluation of the derivative of a Hermite interpolant when the intervals are contiguous and the singletons are located at the endpoints of some or all of the intervals. Consequently, inter-histopolating cardinal functions can be constructed from the Hermite interpolating cardinal functions [30, 48].

THEOREM 6.7. *Suppose given n numbers f_i and n regular and contiguous cells C_i , the first m of which are intervals and the remaining $n - m$, distinct singletons. Suppose that the faces are $-\infty < x_{1/2} < \cdots < x_{m+1/2} < \infty$, and that the intervals*

are ordered in such a way that C_i runs between $x_{i-1/2}$ and $x_{i+1/2}$ for $i = 1, \dots, m$. Finally, let $q \in \mathbb{P}_{n+1}$ be the Hermite interpolant corresponding to the following data:

$$q(x_{1/2}) = 0, \quad (6.1)$$

$$q(x_{i+1/2}) = \sum_{k=1}^i h_k f_k, \quad i = 1, \dots, m, \quad (6.2)$$

$$q'(x_j) = f_j \text{ if } x_j \text{ is a singleton,} \quad (6.3)$$

where h_k is the length of C_k . Then, the inter-histopolant is q' .

Proof. (6.1)–(6.3) make up $1 + m + (n - m) = n + 1$ conditions. Consequently, the corresponding Hermite interpolant q exists and is unique [48]. $q' = f_i$ for i in $m + 1, \dots, n$ by (6.3). It remains to show that the average of q' over C_i equals f_i for $i = 1, \dots, m$; indeed, (6.1) and (6.2) imply that

$$\frac{1}{h_i} \int_{C_i} q' dx = \frac{1}{h_i} (q(x_{i+1/2}) - q(x_{i-1/2})) = \frac{1}{h_i} (h_i f_i) = f_i.$$

□

7. Conversion between arbitrary degrees of freedom and point values.

In this section, we prepare the terrain for the centerpiece of this article, a characterization of superconvergence for linear operators which convert arbitrary degrees of freedom to nodal (point) values by way of polynomial proxies, as well as their inverses. We begin by defining nodal degrees of freedom; then, we define generic degrees of freedom; finally, we define the linear operators which perform the conversions. We also set notation, list elementary properties, and give examples.

7.1. The nodal projection operator π_0^* and the interpolation operator ι_0^* .

DEFINITION 7.1. Given n distinct nodes x_i^* , the associated degrees of freedom, the nodal values, are the point values of functions at the nodes.

DEFINITION 7.2. The nodal projection operator π_0^* is defined as follows: Given a function f , $\pi_0^*(f) \in \mathbb{R}^n$ is the column vector with entries equal to the nodal values $f(x_i^*)$.

DEFINITION 7.3. The interpolation operator ι_0^* is the inverse of the restriction of π_0^* to \mathbb{P}_n , so that $\pi_0^* \iota_0^* = \mathbf{I}$, the identity mapping on \mathbb{R}^n .

ι_0^* maps $\mathbf{f} \in \mathbb{R}^n$ to the unique polynomial $p \in \mathbb{P}_n$ such that $\pi_0^*(p) = \mathbf{f}$. The Greek letters pi (π) and iota (ι) refer to “projection” and “injection” (interpolation being a one-to-one mapping).

DEFINITION 7.4. ℓ_i^* is the Lagrange polynomial corresponding to the i th node, that is, the polynomial of degree $n - 1$ which vanishes at all nodes except x_i^* , where it takes the value 1.

$$\ell_i^* := \prod_{k \neq i} \frac{x - x_k^*}{x_i^* - x_k^*}, \quad i = 1, \dots, n.$$

The Lagrange basis is cardinal with respect to π_0^* , that is, $(\pi_0^* \ell_j^*)_i = \delta_i^j$. We now have two sets of Lagrange polynomials: ℓ_i^* , $i = 1, \dots, n$, which are associated with nodes, and $\ell_{i+1/2}$, $i = 0, \dots, n$, which are associated with faces (§5).

LEMMA 7.5. ι_0^* has a simple formula in terms of the Lagrange polynomials:

$$\iota_0^*(\mathbf{f}) = \sum_{j=1}^n f_j \ell_j^*.$$

7.2. Generic degrees of freedom. We now define abstract degrees of freedom by way of the corresponding projection operator.

DEFINITION 7.6. n degrees of freedom are defined by a linear operator $\pi : \mathbb{P}_{n+1} \rightarrow \mathbb{R}^n$ which is one-to-one on \mathbb{P}_n . (The domain of π may be larger than \mathbb{P}_{n+1} , but no smaller.)

EXAMPLE 2 (Nodal projection). π_0^* is a suitable π .

EXAMPLE 3 (Integral projection). A suitable π is the mapping which, given n intervals C_i with disjoint and nonempty interiors, maps a function f to the integrals $\int_{C_i} f dx$, $i = 1, \dots, n$.

EXAMPLE 4 (Weighted integral projection). A suitable π is the mapping which, given an integrable (weight) function w which is positive almost everywhere, and n intervals C_i with disjoint interiors, maps a function f to the integrals $\int_{C_i} f w dx$, $i = 1, \dots, n$. A further generalization concerns integrals $\int_{C_i} f d\mu$ with μ a positive Borel measure μ , in which case the proof of Theorem 4.1 carries through provided the C_i 's are disjoint open intervals with positive measures [42]. Singletons may be added to the mix as well. Such projection operators arise when solving partial differential equations with highly irregular coefficients, for example, point sources, or discontinuous diffusion coefficients [41].

EXAMPLE 5 (“Average” projection). A suitable π is the mapping which, given n regular cells, maps a function to its “averages.”

EXAMPLE 6 (Point value plus derivatives at a point). A suitable π is $f \mapsto (f(x_0), f'(x_0), f''(x_0), \dots, f^{(n-1)}(x_0)) \in \mathbb{R}^n$.

EXAMPLE 7 (Expansion coefficients). A suitable π is the mapping which associates to a function the first n of its expansion coefficients with respect to some polynomial basis, for example, the first n coefficients of its expansion in terms of Chebyshev (or Legendre) polynomials, or the first n coefficients its Taylor expansion at some point.

EXAMPLE 8 (Point value plus derivatives). A suitable π is the mapping which maps a function to the values of its derivative at $n - 1$ points, together with the value of the function at one point.

EXAMPLE 9. The mapping which maps a function to the values of its derivative at n points is not a suitable π , because constant polynomials are mapped to $\mathbf{0}$.

In the remainder of this article, we assume that π is a linear operator which maps \mathbb{P}_{n+1} into \mathbb{R}^n and which is one-to-one on \mathbb{P}_n , so that it defines n degrees of freedom.

DEFINITION 7.7. ι is the inverse of the restriction of π to \mathbb{P}_n , so that $\pi\iota : \mathbb{R}^n \rightarrow \mathbb{R}^n$ is the identity mapping \mathbf{I} .

LEMMA 7.8. $\iota\pi : \mathbb{P}_{n+1} \rightarrow \mathbb{P}_n$ is a projector onto \mathbb{P}_n , that is,

$$\iota\pi(p) = p \text{ for } p \in \mathbb{P}_n, \quad \text{and} \quad (\iota\pi)(\iota\pi) = \iota\pi.$$

Proof. $(\iota\pi)(\iota\pi) = \iota(\pi\iota)\pi = \iota\mathbf{I}\pi = \iota\pi$. \square

7.3. Generic star operators. ι_0^* maps n nodal values to the unique interpolating polynomial $p \in \mathbb{P}_n$. On the other hand, π maps $p \in \mathbb{P}_n$ to the alternate degrees of freedom. Consequently, $\pi \iota_0^*$ converts nodal degrees of freedom to the other degrees of freedom. Likewise, $\pi_0^* \iota$ converts the other degrees of freedom to nodal values.

LEMMA 7.9. $\pi_0^* \iota$ and $\pi \iota_0^*$ are invertible, and $\pi \iota_0^* = (\pi_0^* \iota)^{-1}$.

Proof. $\iota \pi \iota_0^* = \iota_0^*$ because ι_0^* maps \mathbb{R}^n into \mathbb{P}_n and ι is the inverse of the restriction of π to \mathbb{P}_n . Consequently, $\pi_0^* \iota \pi \iota_0^* = \pi_0^* \iota_0^* = \mathbf{I}$. \square

DEFINITION 7.10.

$$\star := \pi_0^* \iota = (\pi \iota_0^*)^{-1}, \quad \text{and} \quad \star^{-1} := \pi \iota_0^* = (\pi_0^* \iota)^{-1}.$$

\star and \star^{-1} are completely determined by π and π_0^* .

EXAMPLE 10 (Discrete Hodge star operators). *The four discrete Hodge star operators described in Section 1.2.4 are examples of \star 's.*

LEMMA 7.11. *For any choice of distinct nodes, \star is exact on \mathbb{P}_n , that is,*

$$\begin{array}{ccc} \mathbb{P}_n & \xrightarrow{=} & \mathbb{P}_n \\ \pi \downarrow & & \pi_0^* \downarrow \\ \mathbb{R}^n & \xrightarrow{\star} & \mathbb{R}^n \end{array}$$

commutes. (In other words, $\star \pi(p) = \pi_0^(p)$ for every $p \in \mathbb{P}_n$.)*

Proof. ι_0^* is the inverse of the restriction of π_0^* to \mathbb{P}_n . \square

LEMMA 7.12. *For any choice of distinct nodes, \star^{-1} is exact on \mathbb{P}_n , that is,*

$$\begin{array}{ccc} \mathbb{P}_n & \xrightarrow{=} & \mathbb{P}_n \\ \pi_0^* \downarrow & & \pi \downarrow \\ \mathbb{R}^n & \xrightarrow{\star^{-1}} & \mathbb{R}^n \end{array}$$

commutes. (In other words, $\star^{-1} \pi_0^(p) = \pi(p)$ for every $p \in \mathbb{P}_n$.)*

Proof. ι is the inverse of the restriction of π to \mathbb{P}_n . \square

8. Optimal nodes are unique if they exist. At issue is whether exactness can be extended to \mathbb{P}_{n+1} , a form of superconvergence. The following trivial example shows that this is sometimes possible.

EXAMPLE 11. *If $\pi = \pi_0^*$, then $\star = \star^{-1} = \mathbf{I}$, and both stars “convert” point values at n nodes to the exact same degrees of freedom. Consequently, \star and \star^{-1} are not only exact on \mathbb{P}_{n+1} , they are exact on all functions.*

DEFINITION 8.1. *Nodes are said to be optimal (for π) if \star and \star^{-1} are exact on \mathbb{P}_{n+1} .*

EXAMPLE 12. *If $\pi = \pi_0^*$, then the nodes which define π_0^* are optimal (Example 11).*

DEFINITION 8.2.

$$\rho(q) := q - \iota \pi(q).$$

ρ , like ι , is completely determined by π .

LEMMA 8.3. *If $q \in \mathbb{P}_n$, then $\rho(q) = 0$.*

Proof. The restriction of $\iota\pi$ to \mathbb{P}_n is the identity (Lemma 7.8). \square

LEMMA 8.4. $\pi\rho = \mathbf{0}$.

Proof.

$$\pi(\rho(q)) = \pi(q - \iota\pi(q)) = \pi(q) - \pi\iota\pi(q) = \pi(q) - \mathbf{I}\pi(q) = \pi(q) - \pi(q) = \mathbf{0}.$$

\square

LEMMA 8.5. If q is a polynomial of degree n , so is $\rho(q)$.

Proof. The range of ι is \mathbb{P}_n . Consequently, $\iota\pi(q)$ has degree at most $n - 1$. \square

LEMMA 8.6. Let q be a polynomial of degree n , with leading coefficient $c_n \neq 0$. Then, $\rho(q) = c_n\rho(x^n)$. Consequently, $\rho(q)$ and $\rho(x^n)$ have the same roots.

Proof. Because q has degree n , $q = c_n x^n + p$, where $c_n \in \mathbb{R} \setminus \{0\}$ and $p \in \mathbb{P}_n$. Consequently,

$$\begin{aligned} q - \iota\pi(q) &= \{c_n x^n + p\} - \{\iota\pi(c_n x^n) + \iota\pi(p)\} = c_n x^n - \iota\pi(c_n x^n) + p - \iota\pi(p) \\ &= c_n x^n - c_n \iota\pi(x^n) + p - p = c_n \{x^n - \iota\pi(x^n)\}. \end{aligned}$$

\square

The following theorem establishes that both \star and \star^{-1} are exact on \mathbb{P}_{n+1} , a gain of one order, if and only if $\rho(x^n)$ has n simple real roots, and the nodes which define π_0^* are these roots. (Recall that the nodes must be distinct, for otherwise π_0^* is not one-to-one on \mathbb{P}_n , in which case ι_0^* and \star^{-1} are not defined.)

THEOREM 8.7. The following conditions are equivalent:

(a): \star is superconvergent, that is, the following diagram is commutative:

$$\begin{array}{ccc} \mathbb{P}_{n+1} & \xrightarrow{=} & \mathbb{P}_{n+1} \\ \pi \downarrow & & \pi_0^* \downarrow \\ \mathbb{R}^n & \xrightarrow{\star} & \mathbb{R}^n \end{array} . \quad (8.1)$$

(In other words, $\star\pi(p) = \pi_0^*(p)$ for every $p \in \mathbb{P}_{n+1}$.)

(b): \star^{-1} is superconvergent, that is, that is, the following diagram is commutative:

$$\begin{array}{ccc} \mathbb{P}_{n+1} & \xrightarrow{=} & \mathbb{P}_{n+1} \\ \pi_0^* \downarrow & & \pi \downarrow \\ \mathbb{R}^n & \xrightarrow{\star^{-1}} & \mathbb{R}^n \end{array} . \quad (8.2)$$

(In other words, $\star^{-1}\pi_0^*(p) = \pi(p)$ for every $p \in \mathbb{P}_{n+1}$.)

(c): There exists a polynomial p of degree n such that

$$\pi(p) = \pi_0^*(p) = \mathbf{0}. \quad (8.3)$$

(d): The nodes are the (simple) roots of every polynomial q of degree n such that

$$\pi(q) = \mathbf{0}.$$

(e): The nodes are the (simple) roots of $\rho(q)$ for some polynomial q of degree n .

(f): $\rho(q)$ vanishes at the nodes for every polynomial $q \in \mathbb{P}_{n+1}$.

(g): The nodes are the roots of $\rho(x^n)$.

Proof.

(a) \Rightarrow (b): If $p \in \mathbb{P}_{n+1}$, $\star^{-1}\pi_0^*(p) = \star^{-1}\star\pi(p) = \pi(p)$.

(b) \Rightarrow (a): If $p \in \mathbb{P}_{n+1}$, $\star\pi(p) = \star\star^{-1}\pi_0^*(p) = \pi_0^*(p)$. (Note that (8.2) is the “mirror image” of (8.1).)

(a) \Rightarrow (c): Let q have degree n . Then, $p = \rho(q)$ has degree n by Lemma 8.5, $\pi(p) = \mathbf{0}$ by Lemma 8.4, and

$$\pi_0^*(p) = \pi_0^*(q) - \pi_0^*\iota\mathbf{0} = \pi_0^*(q) - \pi_0^*\iota\pi(q) = \pi_0^*(q) - \star\pi(q) = \pi_0^*(q) - \pi_0^*(q) = \mathbf{0}.$$

(c) \Rightarrow (d): Let p be a polynomial of degree n such that (8.3) holds, and q be a polynomial of degree n such that $\pi(q) = \mathbf{0}$. Because $\pi(p) = \pi(q) = \mathbf{0}$, $p = \rho(p)$ and $q = \rho(q)$, so that Lemma 8.6 implies that p and q have the same roots. Consequently, q vanishes at the nodes. Because q has degree n , the nodes are the only roots, and they are simple.

(d) \Rightarrow (e): Because there are n distinct nodes, it is sufficient to show that there exists a polynomial q of degree n such that $\pi(q) = \mathbf{0}$. $q = \rho(x^n)$ has degree n by Lemma 8.5, and $\pi(q) = \pi\rho(x^n) = \mathbf{0}$ by Lemma 8.4.

(e) \Rightarrow (f): If the degree of q is less than n , then $\rho(q)$ vanishes by Lemma 8.3. If q has degree n , $\rho(q)$ and $\rho(x^n)$ have the same roots by Lemma 8.6. Consequently, these roots are independent of q .

(f) \Rightarrow (g): $\rho(x^n)$ has at most n roots and vanishes at n distinct nodes.

(g) \Rightarrow (a): Because \star is linear and exact on \mathbb{P}_n , it is sufficient to show that $\star\pi(p) = \pi_0^*(p)$ for one polynomial p of degree n . Consider $p = \rho(x^n)$. $\pi_0^*(p) = \mathbf{0}$ because the nodes are located at the roots of $\rho(x^n)$. On the other hand, $\pi(p) = \mathbf{0}$ by Lemma 8.4, so that $\star\pi(p) = \mathbf{0}$ as well. \square

COROLLARY 8.8. For a given π , the optimal nodes are unique if they exist.

Proof. The optimal nodes, if they exist, are located at the roots of $\rho(x^n)$, which is completely defined by π . \square

9. Superconvergent conversion between point values and expansion coefficients. To illustrate the generality of the above results, we make a brief detour through polynomial expansions.

Let $\{p_0, p_1, \dots, p_{n-1}\}$ be a basis of \mathbb{P}_n , and let p_n be a polynomial of degree n , so that $\{p_0, p_1, \dots, p_{n-1}, p_n\}$ is a basis of \mathbb{P}_{n+1} . Every polynomial in \mathbb{P}_{n+1} can be uniquely written as $q = \sum_{k=0}^n c_k p_k$. Consequently, the mapping which maps $q \in \mathbb{P}_{n+1}$ to $(c_0, c_1, \dots, c_{n-1}) \in \mathbb{R}^n$ is a suitable π . Furthermore,

$$\iota((c_0, c_1, \dots, c_{n-1})) = \sum_{k=0}^{n-1} c_k p_k, \quad \iota\pi\left(\sum_{k=0}^n c_k p_k\right) = \sum_{k=0}^{n-1} c_k p_k, \quad \text{and } \rho(p_n) = p_n.$$

By Theorem 8.7, the corresponding \star and \star^{-1} are exact on \mathbb{P}_{n+1} if and only if p_n has n simple real roots and the nodes are located there.

EXAMPLE 13. Suppose that $\{p_0, p_1, \dots, p_n\} = \{1, x, x^2, \dots, x^n\}$, so that π corresponds to evaluation of the first n coefficients of the Taylor polynomial based at the origin. Then, $p_n = x^n$ has only one zero, and consequently \star and \star^{-1} cannot be made superconvergent for $n > 1$. (Likewise, the star operator which corresponds to the evaluations of a function and its first $n - 1$ derivatives at some point cannot be made superconvergent.)

EXAMPLE 14. Consider an operator which converts between n point values and the first n (“spectral”) expansion coefficients [9]. That is, suppose that $\{p_0, p_1, \dots, p_n\}$ are polynomials orthogonal with respect to some weight, with $p_k \in \mathbb{P}_n$ for $k < n$ and p_n having degree n , and let \star be the operator which maps n point values to the coefficients

of the interpolating polynomial with respect to this basis. Then, the optimal nodes are the n simple real roots of p_n , hence are those which maximize the order of Gaussian integration [9, 17]. For example, the mapping between point values at the roots of the Chebyshev polynomial of degree n and the first n coefficients of the Chebyshev expansion is superconvergent, and so is its inverse. Likewise for transforms based on Legendre and other orthogonal polynomials.

10. Superconvergent conversion between combinations of point values and cell averages and/or integrals, and nodal values. In this section, we establish the existence of optimal nodes when the projection π maps a function to its “averages” over regular cells (Example 5). We also give a method of computing the optimal nodes without solving the corresponding inter-histopolation problem, in the case when the cells are contiguous.

10.1. “Histograms” with or without gaps.

THEOREM 10.1. *Let n regular cells C_i ’s be given, so that π —the operator which associates to a continuous function its “averages”—is one-to-one on \mathbb{P}_n , and ι , the inverse of π ’s restriction to \mathbb{P}_n , is the operator which maps n cell “averages” to a polynomial inter-histopolant. Then, $\rho(x^n)$ has n simple real roots, which, chosen as nodes, make \star and \star^{-1} superconvergent. Furthermore, every C_i contains a root of $\rho(x^n)$, so that singleton points are optimal nodes, and the other optimal nodes are found in the interior of the cells with positive lengths.*

Proof. Let $p := \rho(x^n)$, so that $\pi(p) = \mathbf{0}$ by Lemma 8.4. If C_i is the singleton x_i , $p(x_i) = (\pi(p))_i = 0$, and x_i must be a root of p . If C_i has length $h_i > 0$, $\int_{C_i} p dx = h_i (\pi(p))_i = 0$, and p must have a root in the interior of C_i . Because the cells are regular, the corresponding roots are distinct. The result follows from Theorem 8.7. \square

What Theorem 10.1 tells us: if p is a polynomial of degree n which vanishes at every singleton and which averages to zero over every cell which is a nontrivial interval—such a polynomial always exists if the cells are regular—then the optimal nodes are located at the (automatically simple) roots of p .

10.2. “Histograms” with contiguous cells. When the cells are contiguous, we can compute the roots of $\rho(x^n) = x^n - \iota\pi(x^n)$ without (directly) computing $\iota\pi(x^n)$.

THEOREM 10.2. *Suppose that the cells C_i , $i = 1, \dots, m \leq n$, are contiguous bounded intervals with disjoint interiors, ordered so that C_i runs from $x_{i-1/2}$ to $x_{i+1/2}$, and that the singletons C_i , $i = m + 1, \dots, n$, are $n - m$ distinct endpoints of these intervals. Then, the optimal nodes are the roots of q' , where*

$$q = \prod_{i=1}^{m+1} (x - x_{i-1/2})^{\alpha_{i-1/2}}, \quad (10.1)$$

and $\alpha_j = 2$ when $\{x_j\}$ is one of the singletons, and $\alpha_j = 1$ otherwise.

Proof. q is a polynomial of degree $n + 1$ because there are $m + 1$ endpoints and $n - m$ singletons, so that $\sum_{i=1}^{m+1} \alpha_{i-1/2} = n + 1$. Consequently, q' has degree n .

If C_i is an interval, then $\int_{C_i} q' dx = 0$ because q vanishes at the endpoints of C_i ; consequently, q' has a root in the interior of C_i . If C_i is the singleton $\{x_j\}$, then q' vanishes because x_j is a double root of q . Consequently, $\pi(q') = \mathbf{0}$, so that $q' = \rho(q') \propto \rho(x^n)$ by Lemma 8.6. The result now follows from Theorem 10.1. \square

COROLLARY 10.3. *In addition to the hypotheses of Theorem 10.2, suppose that the cells run between the simple roots of $q \in \mathbb{P}_{m+1}$, and the singletons are located at the simple roots of $p \in \mathbb{P}_{n-m+1}$, with p a divisor of q . Then the optimal nodes are the roots of $(pq)'$.*

11. Existence of superconvergent discrete Hodge star operators. In this section, we show that the first three discrete Hodge star operators listed in the Introduction can always be made superconvergent, whence the fourth is never superconvergent. We also point out the implications for face elements.

11.1. Three of the four discrete Hodge star operators can be made superconvergent.

COROLLARY 11.1. *Consider the following four discrete Hodge star operators:*

- n **to** n : *the discrete Hodge operator which converts n integrals (over contiguous intervals with positive lengths) to n interior nodal values;*
- $(n - 1) + 1$ **to** $(n - 1) + 1$: *the discrete Hodge operator which converts $n - 1$ integrals (over...) and one boundary value to $n - 1$ interior nodal values and one boundary nodal value (at the same boundary point);*
- $(n - 2) + 2$ **to** $(n - 2) + 2$: *the discrete Hodge operator which converts $n - 2$ integrals (over...) and two boundary values to $n - 2$ interior nodal values and two boundary nodal values; and*
- n **to** $(n - 2) + 2$: *the discrete Hodge operator which converts n integrals (over...) to $n - 2$ interior nodal values and two boundary nodal values.*

For any set of faces, one can choose nodes which make any one of the first three discrete Hodge star operators superconvergent. However, because the boundary nodes are not matched by boundary singletons, the n to $(n - 2) + 2$ discrete Hodge star operator is never superconvergent.

Proof. By Theorem 10.1, given any set of faces, there exists a unique set of optimal nodes. Moreover, every singleton is automatically an optimal node, and the remaining optimal nodes are located in the interiors of the cells with positive lengths. Consequently, one can choose the non-singleton nodes so as to make any of the first three discrete Hodge star operators superconvergent. However, because there are no singletons in the fourth, n to $(n - 2) + 2$, case, no optimal node is located at the boundary, which clashes with the boundary points being nodes. \square

12. Superconvergent discrete Hodge star operators on the interval $[-1, 1]$. In this section, we consider discrete Hodge star operators which convert integrals over contiguous cells, cells which cover the interval $[-1, 1]$, to nodal values. We consider cases with singletons at ± 1 , but leave out n to $(n - 2) + 2$ discrete Hodge star operators, which are never exact on \mathbb{P}_{n+1} .

We characterize the optimal nodes when the faces are defined by an extrema and endpoints grid, paying particular attention to dual grids defined by the roots and extremas or Jacobi polynomials, among them the Legendre and Chebyshev polynomials. Jacobi polynomials are also of interest because of their connection to Gauss and Gauss-Lobatto quadrature formulas.

12.1. Optimal nodes for faces located at the zeros of a known polynomial.

DEFINITION 12.1. *The roots grid associated with a polynomial is the grid with points at the roots of the polynomial. The extrema and endpoints grid is the grid with points at ± 1 together with the roots of the derivative of the polynomial [9].*

COROLLARY 12.2. *Suppose that the cells are contiguous and run between the n simple real roots of the polynomial $q \in \mathbb{P}_{n+1}$, which are located in the interval $(-1, 1)$. Then, the optimal nodes are located at the roots of q' if there are no singletons, the roots of $((x+1)q)'$ if the only singleton is located at -1 , the roots of $((x-1)q)'$ if the only singleton is located at 1 , and the roots of $((x^2-1)q)'$ if the only singletons are located at ± 1 .*

12.2. Superconvergent discrete Hodge star operators defined by Jacobi extrema and endpoints grids. Theorem 10.1 and 10.2 and Corollaries 10.3 and 12.2 apply to arbitrary “face grids,” smooth or not. Consequently, “histograms” defined by Jacobi polynomial extrema and endpoints grids always define a unique set of optimal nodes. Are these optimal nodes located at the points of the roots grid? Before we answer this question, let us consider, in Examples 15 to 18, discrete Hodge star operators which convert n integrals over contiguous cells which range between the points of an extrema and endpoints grid, to n point values (no singletons); these are the first discrete Hodge star operators of the above list of four.

EXAMPLE 15 (Extrema and endpoints of P_2). *0 is the only extremum of $P_2 = (3x^2 - 1)/2$, the Legendre polynomial of degree 2. The Legendre extrema and endpoints grid is $\{-1, 0, 1\}$, and the polynomial q of Corollary 12.2 is $P_2' = 3x$. $((x^2 - 1)q)'$ is $3x^2 - 1 = 2P_2$, and consequently the Legendre roots grid (with nodes at $\pm 1/\sqrt{3}$) is optimal.*

EXAMPLE 16 (Extrema and endpoints of T_2). *0 is the only extrema of $T_2 = 2x^2 - 1$, the Chebyshev polynomial of degree 2. In this case, the Chebyshev extrema and endpoints grid is the same as the Legendre extrema and endpoints grids, and consequently the optimal nodes are located at $\pm 1/\sqrt{3}$. The Chebyshev roots grid, on the other hand, has points at $\pm 1/\sqrt{2}$, and consequently the Chebyshev roots grid is not optimal for the Chebyshev extrema and endpoints grid.*

EXAMPLE 17 (Extrema and endpoints of P_3). *The extrema of the Legendre polynomial $P_3 = (5x^3 - 3x)/2$ are $\pm 1/\sqrt{5}$, so that the Legendre extrema and endpoints grid is $\{-1, -1/\sqrt{5}, 1/\sqrt{5}, 1\}$. $q = P_3'$, $((x^2 - 1)q)'$ is $12P_3$, and the Legendre roots grid $\{-\sqrt{3/5}, 0, \sqrt{3/5}\}$ is optimal.*

EXAMPLE 18 (Extrema and endpoints of T_3). *The extrema of the Chebyshev polynomial $4x^3 - 3x$ are $\pm 1/2$. $q = (x^2 - 1)P_3'$, $((x^2 - 1)q)'$ is $48x^3 - 30x = 6x(8x^2 - 5)$, and the optimal nodes are located at 0 and $\pm\sqrt{5/8}$, which are neither the Chebyshev roots (0 and $\pm\sqrt{3}/2$) nor the Legendre roots.*

In the remainder of this section, we establish that the Jacobi polynomials $P_m^{(0,0)} = P_m$, $P_m^{(1,0)}$, $P_m^{(0,1)}$ and $P_m^{(1,1)}$ are the only ones for which the roots grids are optimal for extrema and endpoints grids, under the assumption that the singletons, if any, are located at the endpoints (and that the integrals which define π are unweighted). First, the positive result.

THEOREM 12.3. *Suppose that the C_i 's, $i = 1, \dots, m \leq n$, are contiguous bounded intervals with disjoint interiors, ordered so that C_i runs from $x_{i-1/2}$ to $x_{i+1/2}$, with*

$$-1 = x_{1/2} < x_{3/2} < \dots < x_{m+1/2} = 1.$$

Suppose also that

- (i): $m = n$ (an n to n discrete Hodge star operator in the notation of Corollary 11.1), that is, there are no singletons, and the interior faces are located at the extrema of the Legendre polynomial P_m , or

- (ii): $m = n - 1$ (an $(n - 1) + 1$ to $(n - 1) + 1$ discrete Hodge star operator), the singleton is located at -1 , and the interior faces are located at the extrema of the Jacobi polynomial $P_m^{(0,1)}$, or
- (iii): $m = n - 1$ (an $(n - 1) + 1$ to $(n - 1) + 1$ discrete Hodge star operator), the singleton is located at 1 , and the interior faces are located at the extrema of the Jacobi polynomial $P_m^{(1,0)}$, or
- (iv): $m = n - 2$ (an $(n - 2) + 2$ to $(n - 2) + 2$ discrete Hodge star operator), the singletons are located at ± 1 , and the interior faces are located at the extrema of the Jacobi polynomial $P_m^{(1,1)}$.

Then, the roots grids are optimal, that is, the optimal nodes are located at the roots of P_m in case (i), the roots of $P_m^{(0,1)}$ together with -1 in case (ii), the roots of $P_m^{(1,0)}$ together with 1 in case (iii), and the roots of $P_m^{(1,1)}$ together with ± 1 in case (iv).

Proof. Let (α, β) equal $(0, 0)$ in case (i), $(0, 1)$ in case (ii), $(1, 0)$ in case (iii), and $(1, 1)$ in case (iv). $P_m^{(\alpha, \beta)}$ has $m - 1$ distinct extrema, located in the interval $(1, 1)$, because $P_m^{(\alpha, \beta)}$ has m simple roots there [1, 17]. The polynomial q of Corollary 12.2 is $\frac{d}{dx} P_m^{(\alpha, \beta)}$, and the optimal nodes are located at the roots of

$$\frac{d}{dx} \left\{ (1-x)^{\alpha+1} (1+x)^{\beta+1} \frac{d}{dx} P_m^{(\alpha, \beta)} \right\}.$$

On the other hand, $P_m^{(\alpha, \beta)}$ is the eigenfunction of the Sturm-Liouville problem

$$\frac{d}{dx} \left\{ (1-x)^{\alpha+1} (1+x)^{\beta+1} \frac{dy}{dx} \right\} + \lambda (1-x)^\alpha (1+x)^\beta y = 0$$

corresponding to $\lambda = m(m + \alpha + \beta + 1) \neq 0$ [16]. Consequently, the optimal nodes are the roots of $(1-x)^\alpha (1+x)^\beta P_m^{(\alpha, \beta)}$. \square

We now establish that dual grids based on the roots and extrema of Jacobi polynomials other than the four listed in Theorem 12.3—for example, Chebyshev roots and extrema and endpoints grids—are *not* optimal.

THEOREM 12.4. *Suppose that the C_i 's have positive lengths and are contiguous. Suppose also that the faces are located at the extrema of $P_m^{(\alpha, \beta)}$ together with ± 1 , and that the singletons, if any, are located at the endpoints ± 1 . Finally, suppose that the optimal nodes are located at the roots of $P_m^{(\alpha, \beta)}$. Then, $P_m^{(\alpha, \beta)}$ is one of the four Jacobi polynomials listed in Theorem 12.3.*

Proof. Let $(\hat{\alpha}, \hat{\beta})$ equal $(0, 0)$ if there are no singletons, $(0, 1)$ if the singleton is at -1 , $(1, 0)$ if it is at 1 , and $(1, 1)$ if there are two singletons. By Corollary 12.2, we must have that

$$(1-x)^{\hat{\alpha}} (1+x)^{\hat{\beta}} P_m^{(\alpha, \beta)} \propto \frac{d}{dx} \left\{ (1-x)^{\hat{\alpha}+1} (1+x)^{\hat{\beta}+1} \frac{d}{dx} P_m^{(\alpha, \beta)} \right\}.$$

This implies that $P_m^{(\alpha, \beta)}$ is an eigenfunction of the Sturm-Liouville problem

$$\frac{d}{dx} \left\{ (1-x)^{\hat{\alpha}+1} (1+x)^{\hat{\beta}+1} \frac{dy}{dx} \right\} + \lambda (1-x)^{\hat{\alpha}} (1+x)^{\hat{\beta}} y = 0,$$

so that $\alpha = \hat{\alpha}$ and $\beta = \hat{\beta}$ [23]. \square

13. Nodes are optimal for infinitely many sets of faces. In this section, we indicate why it is preferable to optimize the nodes, not the faces. Briefly, this is because “optimal faces” may not exist, and if they exist, they are not unique.

Consider discrete Hodge star operators which convert integrals over contiguous intervals (no singletons) to n nodal values. By Theorem 10.1, given any set of $n + 1$ (distinct) faces, there exists a unique set of n nodes such that the corresponding discrete Hodge star operator and its inverse are exact on \mathbb{P}_{n+1} . Does the converse hold? That is, given n (distinct) nodes, does there exist a unique set of faces such that \star is exact on \mathbb{P}_{n+1} ? The answer is “No:” If a collection of nodes is optimal for some set of faces, then it is optimal for a one-parameter family of sets of faces. Furthermore, for every $n > 3$, there exists a set of n nodes which is not optimal for any set of faces. The remainder of this section is devoted to illustrating and establishing these facts.

LEMMA 13.1. *Suppose that \star , which converts n integrals over contiguous cells to nodal values, is exact on \mathbb{P}_{n+1} . Suppose also that the optimal nodes are located at the roots of the n th degree polynomial p . Then, the faces are located at the roots of one of the antiderivatives of p .*

Proof. p must be proportional to the derivative of the polynomial q given in (10.1). Consequently, q must be proportional to one of the antiderivatives of p . \square

EXAMPLE 19 ($n = 1$: one-parameter family of “optimal faces”). *Suppose that there is only one node $x_1^* = 0$ ($n = 1$). Because the average of a linear function over a bounded interval with positive length is its value at the center point, \star is exact on \mathbb{P}_2 whenever $x_{1/2} = -x_{3/2}$. Consequently $x_1^* = 0$ is an optimal node for a one-parameter family of faces.*

EXAMPLE 20 ($n = 2$: one-parameter family of “optimal faces”). *Suppose that the nodes are ± 1 , the roots of $p := x^2 - 1$ ($n = 2$). Let $q := x^3/3 + x - c$ be an antiderivative of p . Then, -1 is a local maximum of q and 1 is a local minimum. Because $q(-1) = -4/3 - c$ and $q(1) = 4/3 - c$, q has three simple real roots if and only if $c \in (-4/3, 4/3)$. Consequently, the nodes ± 1 are optimal for a one-parameter family of sets of faces.*

EXAMPLE 21 ($n = 3$: one-parameter family of “optimal faces”). *Suppose that the nodes are $x_1^* < x_2^* < x_3^*$, the roots of $p := (x - x_1^*)(x - x_2^*)(x - x_3^*)$ and let q be an antiderivative of p ($n = 3$). Then, x_1^* and x_3^* are local minimas of q , x_2^* is a local maximum, and $q(x_2^*) > \max(q(x_1^*), q(x_3^*))$. Consequently, $q - c$ has three simple real roots if and only if $c \in (\max(q(x_1^*), q(x_3^*)), q(x_2^*))$. Consequently, the nodes are optimal for a one-parameter family of sets of faces.*

EXAMPLE 22 ($n = 3$: non-existence of “optimal faces”). *Suppose that the nodes are evenly spaced and located at $\pm 1/3$ and ± 1 , the roots of $p := (x^2 - 1)(x^2 - 1/9)$ ($n = 4$). Let $q := x^5/5 - 10x^3/27 + x/9$ be an antiderivative of p . Then, $q - c$ has five simple real roots if and only if $c \in (-88/3645, 88/3645)$. Consequently, the nodes are optimal for a one-parameter family of sets of faces. For example, the faces which correspond to $c = 0$ are $0, \pm\sqrt{25 - 2\sqrt{55}}/(3\sqrt{3}) \approx \pm 0.61$, and $\pm\sqrt{25 + 2\sqrt{55}}/(3\sqrt{3}) \approx 1.2$. For other values of c , the faces are not symmetric about the origin.*

EXAMPLE 23. *Suppose that the nodes are located at $\pm 1/2$ and ± 1 , the roots of $p := (x^2 - 1)(x^2 - 1/4)$ ($n = 4$). Let $q := x^5/5 - 5x^3/12 + x/4$ be an antiderivative of p . No horizontal line crosses the graph of q more than three times, and $q - c$ does not have five real roots for any value of c . Consequently, the nodes are not optimal for any set of faces.*

LEMMA 13.2. *Let p be a polynomial of degree n with real simple roots $x_1^*, x_2^*, \dots, x_n^*$,*

and let q be one of its antiderivatives. Then, one of the vertical translates of q has $n + 1$ simple real roots if and only if

$$a := \max \{q(x_i^*) \text{ such that } q''(x_i^*) > 0\} < b := \min \{q(x_i^*) \text{ such that } q''(x_i^*) < 0\}. \quad (13.1)$$

Furthermore, if (13.1) holds, then $q - c$ has $n + 1$ simple real roots if and only if $c \in (a, b)$.

Proof. Because the roots of p are simple, they are either local minimas of q —if $p'(x_i^*) = q''(x_i^*) > 0$ —or local maximas of q —if $p'(x_i^*) = q''(x_i^*) < 0$ —and they alternate.

If $q - c$ has $n + 1$ distinct real roots, they are simple and consequently distinct from the x_i^* 's. By Rolle's Theorem, there is exactly one root of p between consecutive roots of $q - c$. Because $q - c$ has a constant sign between its roots, we must have that $q(x_i^*) - c < 0$ if x_i^* is a local minimum, and $q(x_i^*) - c > 0$ otherwise. Consequently, $a < c < b$.

Conversely, if (13.1) holds and $a < c < b$, q takes the value c between consecutive nodes, as well as between $-\infty$ and the leftmost node, and between the rightmost node and ∞ . Consequently, $q - c$ has $n + 1$ simple real roots. \square

THEOREM 13.3. Consider star operators which convert $n \geq 2$ integrals over contiguous intervals to n nodal values. Suppose that the n nodes $x_1^*, x_2^*, \dots, x_n^*$ are the simple roots of the n th degree polynomial p , and let q be an antiderivative of p . Then, there exist $n + 1$ distinct faces for which the nodes are optimal if and only if the largest local minimum of q is smaller than its smallest local maximum, that is, if (13.1) holds. Furthermore, the nodes are optimal if the faces are located at the roots of $q - c$ for every $c \in (a, b)$, and for other values of c , $q - c$ does not have $n + 1$ simple real roots.

Proof. Lemmas 13.1 and 13.2. \square

COROLLARY 13.4. Consider star operators which convert n integrals over contiguous intervals to n nodal values. For any $n > 3$, there exists a set of n distinct nodes which is not optimal for any set of $n + 1$ distinct faces.

Proof. For every $n > 3$, there exists a polynomial q of degree $n + 1$ with simple roots and a local minimum larger than a local maximum. The extrema of q define a set of nodes which are not optimal for any set of faces. \square

14. Discrete star operators which convert n integrals or averages to n nodal values. In this section, we focus on discrete star operators which convert n integrals or averages, over contiguous intervals with positive lengths (no singletons), to n nodal values, and their inverses. This includes the n to n and n to $(n - 2) + 2$ discrete Hodge star operators.

14.1. The cells C_i , the faces x_j , and the nodes x_i^* . In the remainder of this article, the cells C_i are n contiguous intervals with disjoint interiors and lengths $0 < h_i < \infty$. Consequently, the cells are defined by the locations of $n + 1$ faces, which we order so that C_i runs from $x_{i-1/2}$ to $x_{i+1/2}$, where $-\infty < x_{1/2} < \dots < x_{n+1/2} < \infty$. The nodes are n distinct real numbers, ordered so that $-\infty < x_1^* < \dots < x_n^* < \infty$.

14.2. The projection operators π (cell masses) and $\bar{\pi}$ (cell averages). The degrees of freedom associated with cells, the *masses*, or *integrals*, are the integrals of functions over the n cells. Associated with these degrees of freedom are projection operators. The *integral projection* operator π is defined as follows: Given an integrable function f , $\pi(f) \in \mathbb{R}^n$ is the column vector with entries the masses $\int_{C_i} f dx$ (Example

3). The *average projection* $\bar{\pi}$ is defined similarly: Given an integrable function f , $\bar{\pi}(f) \in \mathbb{R}^n$ is the column vector with entries the averages $\frac{1}{h_i} \int_{C_i} f dx$ [32, 39, 41, 56].

14.3. The histopolation operators ι and $\bar{\iota}$. Let ι (resp. $\bar{\iota}$) be the inverse of π 's (resp. $\bar{\pi}$'s) restriction to \mathbb{P}_n , so that ι (resp. $\bar{\iota}$) associates a histopolating polynomial in \mathbb{P}_n to every column vector $\mathbf{f} \in \mathbb{R}^n$. ι is a right inverse of π , that is, $\pi\iota = \mathbf{I}$; likewise for $\bar{\iota}$: $\bar{\pi}\bar{\iota} = \mathbf{I}$ (Theorem 4.1). The histopolating cardinal functions (Theorem 5.2) provide closed forms for the histopolation operators:

$$\iota(\mathbf{f}) = \sum_{j=1}^n f_j \varrho_j, \quad \bar{\iota}(\mathbf{f}) = \sum_{j=1}^n f_j \bar{\varrho}_j.$$

14.4. \star , the discrete Hodge star operator from masses to nodal values, and $\bar{\star}$, which maps averages. The discrete Hodge operator \star is defined as follows: $\star := \pi_0^* \iota$; this corresponds to histopolating (ι), then evaluating the histopolant at the nodes (π_0^*). Equivalently, \star is the unique mapping which makes the following diagram commutative

$$\begin{array}{ccc} \mathbb{P}_n & \xrightarrow{=} & \mathbb{P}_n \\ \pi \downarrow & & \pi_0^* \downarrow \\ \mathbb{R}^n & \xrightarrow{\star} & \mathbb{R}^n \end{array} \quad (14.1)$$

(Lemma 7.11). (The “=” at the top of diagram (14.1) corresponds to the *continuum* Hodge star operator from 1- to 0-forms [39].) $\bar{\star}$, which maps averages to nodal values, is defined analogously: $\bar{\star} := \pi_0^* \bar{\iota}$. Following are closed form formulas for the entries of \star and $\bar{\star}$ in terms of the nodal values of histopolating cardinal basis polynomials:

$$[\star]_{ij} = \varrho_j(x_i^*), \quad [\bar{\star}]_{ij} = \bar{\varrho}_j(x_i^*), \quad (14.2)$$

so that

$$\bar{\star} = \star \mathbf{H},$$

where \mathbf{H} is the diagonal matrix of cell lengths h_i .

14.5. \star^{-1} , the discrete Hodge star operator from nodal values to masses, and $\bar{\star}^{-1}$, which maps to averages. \star and $\bar{\star}$ are invertible. The discrete Hodge operator \star^{-1} —the inverse of \star —is $\pi \iota_0^*$ (Lemma 7.9). This corresponds to interpolating (ι_0^*), then integrating the interpolant over the cells (π). Equivalently, \star^{-1} is the unique mapping which makes the following diagram commutative:

$$\begin{array}{ccc} \mathbb{P}_n & \xrightarrow{=} & \mathbb{P}_n \\ \pi_0^* \downarrow & & \pi \downarrow \\ \mathbb{R}^n & \xrightarrow{\star^{-1}} & \mathbb{R}^n \end{array} \quad (14.3)$$

(Lemma 7.12). (The “=” in diagram (14.3) corresponds to the *continuum* Hodge star operator from 0- to 1-forms.) $\bar{\star}^{-1}$ —the inverse of $\bar{\star}$ —which maps nodal values to averages, can be defined analogously: $\bar{\star}^{-1} := \pi \iota_0^*$. Following are closed form formulas

for the matrix entries of \star^{-1} and $\bar{\star}^{-1}$ in terms of cell integrals of nodal Lagrange polynomials (Definition 7.4):

$$[\star^{-1}]_{ij} = \int_{C_i} \ell_j^* dx, \quad [\bar{\star}^{-1}]_{ij} = \frac{1}{h_i} \int_{C_i} \ell_j^* dx. \quad (14.4)$$

With the help of a computer algebra system, it is not difficult to obtain the entries of the discrete star matrices from formulas (14.2) and (14.4) [9, 40, 47]. Very compact code can be written by calling on polynomial differentiation packages and real polynomial root finders.

15. Tested grids. In the remainder of this article, we present numerical results pertaining discrete star operator which maps n averages to n nodal values, and its inverse. We consider a number of dual grids with cells which cover the interval $[-1, 1]$:

Uniform grid: The (plain) uniform dual grid has $n + 1$ equidistant faces—so that the cells have lengths $h = 2/n$ —and equidistant nodes, located at the centers of the cells [39, 41]. These nodes are not optimal for this choice of cell faces.

Optimized uniform grid: The optimized uniform dual grid has the same faces as the uniform grid: $x_{j+1/2} = -1 + jh$, $j = 0, \dots, n$. However, the nodes are located at the extrema of $\prod_{j=0}^n (x - x_{j+1/2})$. These nodes are optimal (Theorem 10.2).

Chebyshev grid: The (plain) Chebyshev dual grid has faces at the Chebyshev extrema and endpoints grid, and nodes at the Chebyshev roots grid. That is, the faces are located at ± 1 together with the extrema of T_n , the nodes, at the roots of T_n [9]. The nodes are not optimal (Theorem 12.4).

Optimized Chebyshev grid: The optimized Chebyshev dual grid has faces at the Chebyshev extrema and endpoints grid, like the plain Chebyshev grid. However, instead of being located at the roots of the Chebyshev polynomial T_n , the nodes are located at the extrema of $(x^2 - 1)T'_n$. The nodes are optimal (Corollary 12.2).

Legendre grid: The (plain) Legendre dual grid has faces at the Legendre extrema and endpoints grid and nodes at the Legendre roots grid [9]. The nodes are optimal (Theorem 12.3).

16. The condition number of $\bar{\star}$. The assertions made in the remainder of the article should be interpreted as conjectures, since they are based on numerical evidence.

Figure 16.1 shows the condition numbers κ_2 of $\bar{\star}$ (and $\bar{\star}^{-1}$) as functions of the number n of nodes and cells for the various grids. Most notably, the Legendre and plain and optimized Chebyshev κ_2 s appear to be less than 2 for all n . Also, the condition numbers for optimized grids are smaller than for their plain counterparts, the exception being the plain uniform grid, which yields the smallest condition number for $n < 4$.

17. $\bar{\star}$ and $\bar{\star}^{-1}$ are close to the identity. Identifying averages with nodal values is a first order approximation if the nodes are in or near the corresponding cells, a second order approximation if the nodes are located at the cell centers [41]. For this reason, the identity matrix \mathbf{I} is a first order star operator for all the above dual grids, and a second order star operator for the plain uniform dual grid. One consequently expects the higher-order star operators defined by the above dual grids to be close to the identity. Figure 17.1 shows the matrix (operator) 2-norms of the differences between the identity matrix \mathbf{I} and the star operators $\bar{\star}$ and $\bar{\star}^{-1}$ for the

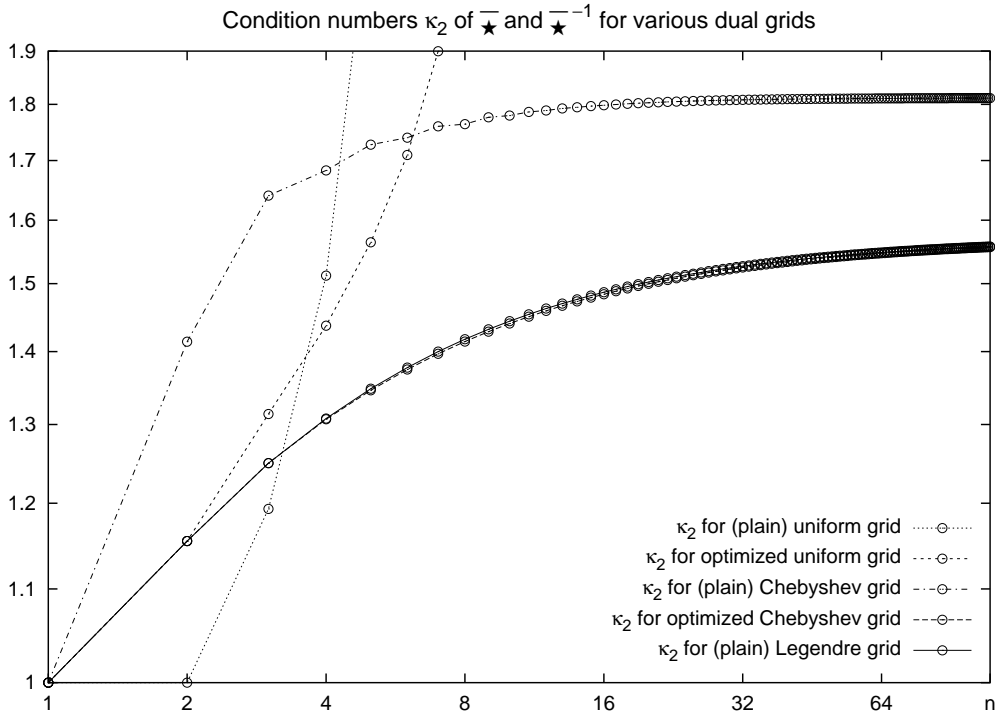


Fig. 16.1: Condition numbers κ_2 of $\bar{\star}$ and $\bar{\star}^{-1}$ for various dual grids, as functions of the number n of degrees of freedom. From bottom (best) to top (worst): optimized Chebyshev grid, (plain) Legendre grid (almost indistinguishable from the optimized Chebyshev grid), (plain) Chebyshev grid, optimized uniform grid (off the chart for $n > 7$) and (plain) uniform grid (off the chart for $n > 4$). When $n = 1$, all condition numbers equal 1 because $\bar{\star} = \mathbf{I}$ (for the plain uniform grid, $\bar{\star} = \mathbf{I}$ when $n = 2$ as well). With the exception of the uniform grid κ_2 for $n < 4$, the optimized grids yield smaller condition numbers than their plain counterparts. It appears that, asymptotically, $\kappa_2 \approx 1.8$ for the plain Chebyshev grid, and $\kappa_2 \approx 1.6$ for the optimized Chebyshev and Legendre grids. κ_2 for the plain and optimized uniform grids diverge (when $n = 16$, κ_2 is about 400 for the optimized uniform grid and 300000 for the plain uniform grid). Not shown: The condition numbers k_1 and k_∞ for the Legendre and optimized Chebyshev grids approximately equal 1.7 when n is large. For the plain Chebyshev grid, the condition number k_1 appears to be bounded, but k_∞ diverges.

various grids. For the Legendre and both Chebyshev grids, $\|\mathbf{I} - \bar{\star}\|_2 < 1$ for all n ; $\|\mathbf{I} - \bar{\star}^{-1}\|_2$ is particularly small: about .4 for the Legendre and optimized Chebyshev grids, .5 for the plain Chebyshev grid. Star operators based on uniform grids diverge as $n \rightarrow \infty$. In any case, for $n > 4$, the optimized grids yield star operators closer to the identity than their plain counterparts.

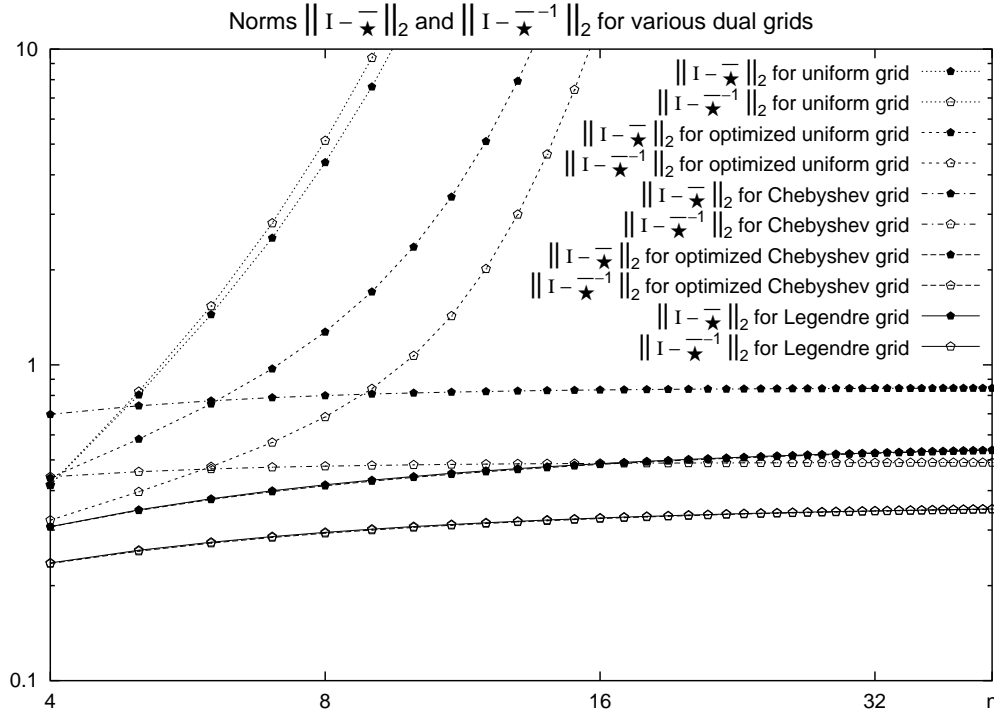


Fig. 17.1: Matrix 2-norms of the differences between the identity matrix \mathbf{I} and the star operators $\bar{\star}$ and $\bar{\star}^{-1}$, as functions of the number n of degrees of freedom. From bottom (best) to top (worst): optimized Chebyshev grid, Legendre grid (almost indistinguishable from the optimized Chebyshev grid), Chebyshev grid, optimized uniform grid, and uniform grid. For the Legendre and both Chebyshev grids, $\|\mathbf{I} - \bar{\star}\|_2$ and $\|\mathbf{I} - \bar{\star}^{-1}\|_2$ are less than 1 for all n . $\|\mathbf{I} - \bar{\star}^{-1}\|_2$, in particular, is small: about .4 for the Legendre and optimized Chebyshev grids, .5 for the plain Chebyshev grid. $\bar{\star}$ and $\bar{\star}^{-1}$ diverge for both uniform grids.

18. Test functions. In the remainder of this article, we perform numerical convergence tests for four test functions:

e^x : The exponential function e^x , which is entire.

$1/(1+x^2)$: The Lorentzian or Witch of Agnesi function, which is analytic on the interval $[-1, 1]$, with poles at $\pm i$ [9].

$1/(1+25x^2)$: A variant of the Witch of Agnesi, also analytic on the interval $[-1, 1]$, with poles at $\pm i/5$. The polynomials which interpolate $1/(1+25x^2)$ at the faces of the plain and optimized uniform grids diverge pointwise for $|x| > .73$ as $n \rightarrow \infty$ [26].

Heaviside (unit step): The Heaviside, or unit step, function, which is discontinuous, equals 0 for $x < 0$, $1/2$ for $x = 0$, and 1 for $x > 0$.

19. Errors. For every test function f , and every grid, we compute the MAX and RMS norms of $\pi_0^*(f) - \star \bar{\pi}(f)$ and $\bar{\pi}(f) - \star^{-1} \pi_0^*(f)$.

19.1. MAX errors. $\pi_0^*(f) - \star \bar{\pi}(f)$ is the difference between the exact nodal values of f ($\pi_0^*(f)$) and those reconstructed by \star from the cell averages of f . The MAX \star error is defined as

$$\max_{i=1,\dots,n} |[\pi_0^*(f)]_i - [\star \bar{\pi}(f)]_i| = \max_{i=1,\dots,n} |[\pi_0^*(f - \bar{\iota} \bar{\pi}(f))]_i|.$$

The MAX $\bar{\star}$ error approximates the sup norm of $f - \bar{\iota} \bar{\pi}(f)$. $f - \bar{\iota} \bar{\pi}(f)$ is the difference between f and the histopolant reconstructed from f 's cell averages.

$\bar{\pi}(f) - \star^{-1} \pi_0^*(f)$ is the difference between the exact cell averages of f ($\bar{\pi}(f)$) and those reconstructed by \star^{-1} from the nodal values of f . The MAX $\bar{\star}^{-1}$ error is

$$\max_{i=1,\dots,n} |[\bar{\pi}(f)]_i - [\star^{-1} \pi_0^*(f)]_i| = \max_{i=1,\dots,n} |[\bar{\pi}(f - \iota_0^* \pi_0^*(f))]_i|.$$

The MAX $\bar{\star}^{-1}$ error approximates the sup norm of $f - \iota_0^* \pi_0^*(f)$, the difference between f and the interpolant reconstructed from f 's nodal values.

Because $\bar{\star}^{-1}$ is the inverse of \star , the truncation error of the former is the solution error of the latter, and vice versa.

19.2. RMS errors. The RMS $\bar{\star}$ error is defined as

$$\left\{ \frac{1}{2} \sum_{i=1}^n h_i ([\pi_0^*(f)]_i - [\star \bar{\pi}(f)]_i)^2 \right\}^{1/2} = \left\{ \frac{1}{2} \sum_{i=1}^n h_i ([\pi_0^*(f - \bar{\iota} \bar{\pi}(f))]_i)^2 \right\}^{1/2}.$$

The 1/2 scaling is so that the RMS error equal the MAX error when the error $\pi_0^*(f - \bar{\iota} \bar{\pi}(f))$ is constant. The RMS \star error approximates $\sqrt{2}$ times the \mathbb{L}^2 norm of $f - \bar{\iota} \bar{\pi}(f)$.

The RMS $\bar{\star}^{-1}$ error is

$$\left\{ \frac{1}{2} \sum_{i=1}^n h_i ([\bar{\pi}(f)]_i - [\star^{-1} \pi_0^*(f)]_i)^2 \right\}^{1/2} = \left\{ \frac{1}{2} \sum_{i=1}^n h_i ([\bar{\pi}(f - \iota_0^* \pi_0^*(f))]_i)^2 \right\}^{1/2}.$$

The RMS $\bar{\star}^{-1}$ error approximates $\sqrt{2}$ times the \mathbb{L}^2 norm of $f - \iota_0^* \pi_0^*(f)$.

19.3. Error ratios. To facilitate the comparison between the performances of star operators corresponding to different grids, in particular the discrete star operators corresponding to plain and optimized grids based on the same set of faces, we present plots of errors normalized by the errors obtained for Legendre grid star operators. These are the errors for the star operators corresponding to the various grids divided by the errors for the star operators corresponding to the Legendre grid. Superconvergence is most easily identified by comparing such normalized errors.

20. Numerical convergence tests.

20.1. RMS errors for discrete star operators based on Legendre grids.

The discrete star operators based on Legendre grids are the best overall. (The ones based on optimized Chebyshev grids are almost as good.) In Figure 20.1, we show, for all test functions, the RMS errors for discrete star operators based on Legendre grids. The computed averages and nodal values converge exponentially for the three analytic test functions, with slower convergence as poles approach $[-1, 1]$. For the discontinuous test function, the averages and nodal values converge at order 1/2.

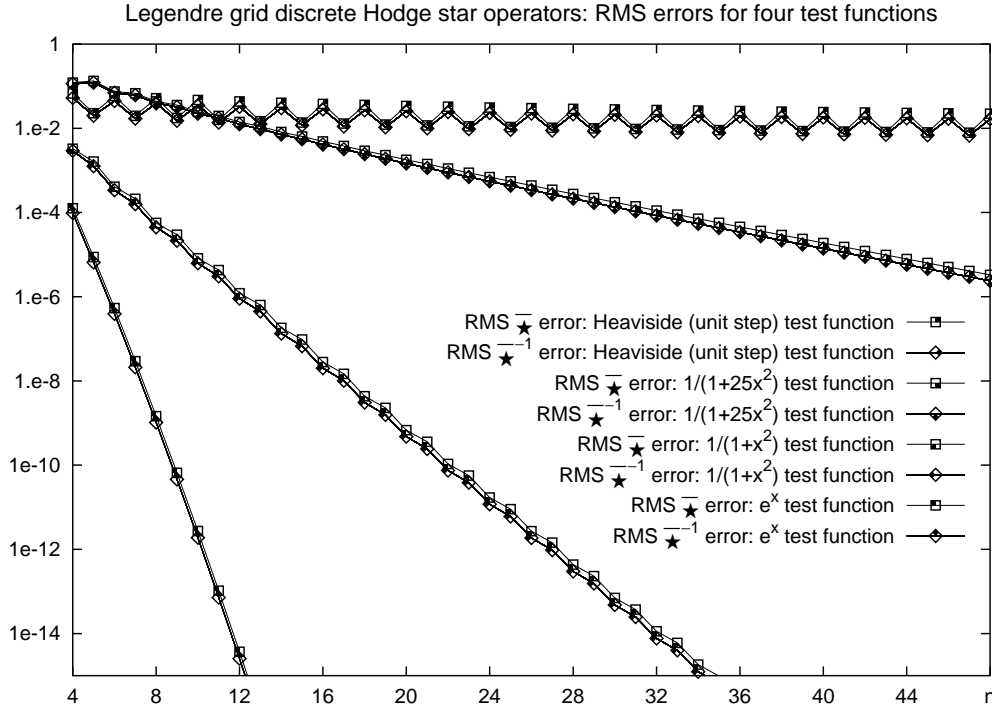


Fig. 20.1: Legendre grid $\bar{\star}$ and $\bar{\star}^{-1}$ RMS errors, as functions of the number n of degrees of freedom, for all test functions. From bottom (smallest errors) to top (largest errors): e^x , $1/(1+x^2)$, $1/(1+25x^2)$ and Heaviside (unit step). Exponential convergence is seen for the analytic test functions, with decreasing rates as singularities approach the interval. (See [9] for a discussion of how various convergence rates manifest themselves in error plots.) Errors computed using the arbitrary precision arithmetic package of the computer algebra system AXIOM [34, 40].

20.2. Results for the test function e^x . Figures 20.2 and 20.3 show the errors obtained over the various grids for the test function e^x . The figures show that the cell averages and nodal values computed with $\bar{\star}$ and $\bar{\star}^{-1}$ converge exponentially in MAX and RMS norms for all grids. The same errors, normalized by the corresponding Legendre grid errors, are shown in Figure 20.4. One sees that the optimized versions of the uniform and Chebyshev grids yield much smaller errors than their plain counterparts. For large n , the optimized Chebyshev grid MAX errors are about $\mathbf{O}(1/n^2)$ relative to the plain Chebyshev errors, and the RMS errors, $\mathbf{O}(1/n)$. This validates the superconvergence claims, since it indicates that averages and nodal values computed with optimized nodes converge at one or two orders faster than those computed with non-optimized nodes. Also notable is that the errors for the optimized Chebyshev grids are almost the same as the errors for the Legendre grids.

20.3. Results for the test function $1/(1+x^2)$. Figure 20.5 shows the errors for the test function $1/(1+x^2)$. The averages and nodal values converge exponentially

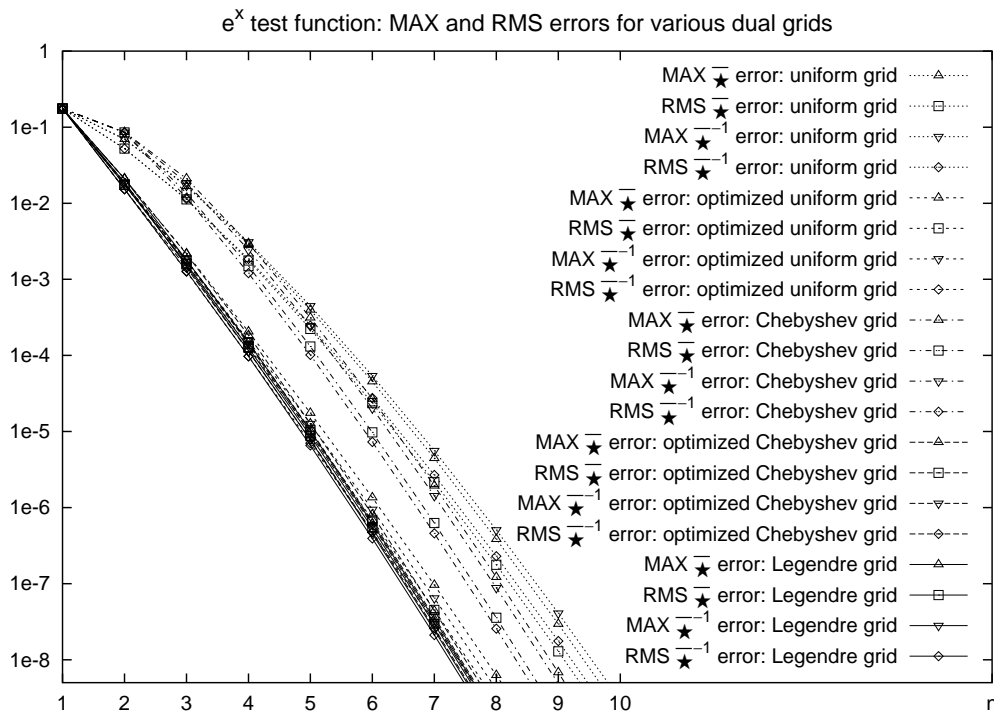


Fig. 20.2: Test function: e^x . MAX (\triangle) and RMS (\square) errors for the nodal point values computed with \star , and MAX (∇) and RMS (\diamond) errors for the cell averages computed with \star^{-1} , as functions of the number n of degrees of freedom, for all grids. The key to plotting symbols is used for all subsequent plots.

in MAX and RMS norms for all grids, although less rapidly than for e^x . Errors normalized by the Legendre grid errors are shown in Figure 20.6. Again, the errors are smallest for the Legendre and optimized Chebyshev grids. Superconvergence is still observed: The MAX errors for the optimized Chebyshev grid are $\mathbf{O}(1/n)$ relative to the errors for the plain Chebyshev grid.

20.4. Results for the test function $1/(1+25x^2)$. Figure 20.7 shows the errors for the test function $1/(1+25x^2)$. Although the averages and nodal values converge exponentially in MAX and RMS norms for the Legendre and the plain and optimized Chebyshev grids, they diverge for the plain and optimized uniform grids (this is not surprising given that the corresponding interpolants diverge). The Legendre and optimized Chebyshev grids still are best but the plain Chebyshev grid is almost as good.

20.5. Results for the Heaviside (unit step) test function. Figure 20.8 shows the errors for the test function $1/(1+25x^2)$. Algebraic convergence is observed: RMS errors for the Legendre and plain and optimized Chebyshev grids are $\mathbf{O}(1/\sqrt{n})$. MAX errors, on the other hand, appear to converge to about 7% of the size of the jump. The average and nodal values computed by the plain and optimized uniform

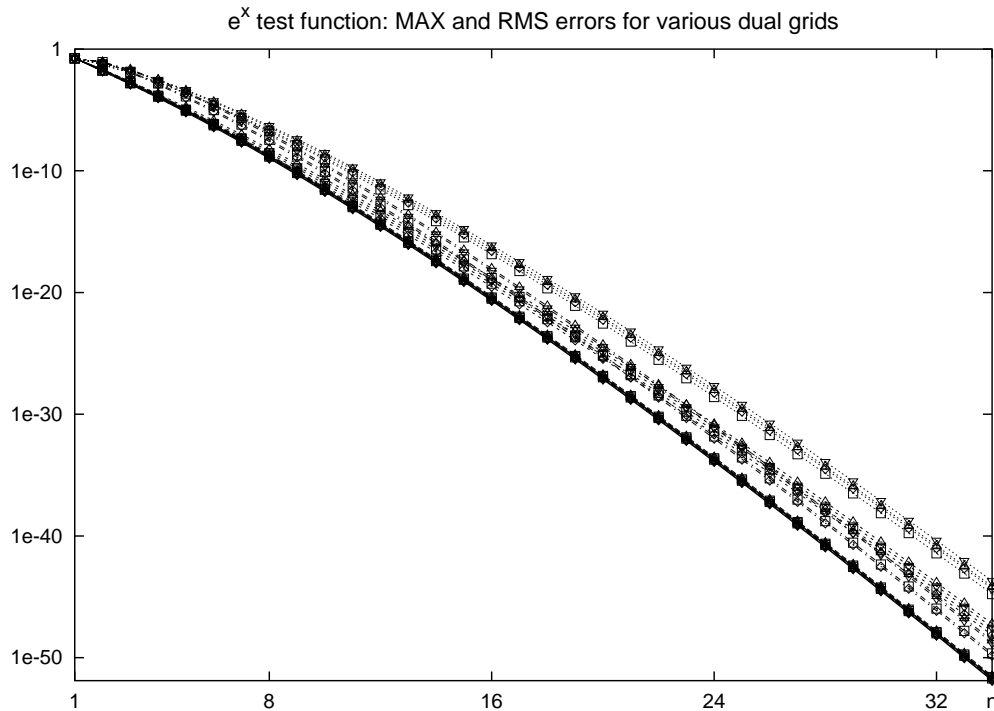


Fig. 20.3: Test function: e^x . MAX and RMS errors, as functions of the number n of degrees of freedom, for all grids. See Figure 20.2 for the key. The nodal and average values computed by \star and its inverse converge exponentially, possibly supergeometrically, for all grids [9].

grids discrete star operators diverge.

Acknowledgements. I am grateful for the feedback and suggestions of Bob Russell, Stanly Steinberg, Wentao Sun, Manfred Trummer and Jim Verner. I also thank Peter Borwein, Thomas Hagstrom, Claudio Mattiussi, Robert McLachlan and Fernando Teixeira for useful conversations, as well as IBM and NAG for making the computer algebra system AXIOM available to the community.

REFERENCES

- [1] M. ABRAMOWITZ AND I. A. STEGUN, eds., *Handbook of mathematical functions with formulas, graphs, and mathematical tables*, Dover Publications Inc., New York, 1992. Reprint of the 1972 edition.
- [2] D. N. ARNOLD, *Differential complexes and numerical stability*, in Proceedings of the International Congress of Mathematicians, Beijing 2002, 2002.
- [3] A. BOSSAVIT, *Mixed finite elements and the complex of Whitney forms*, in The mathematics of finite elements and applications, VI (Uxbridge, 1987), Academic Press, London, 1988, pp. 137–144.
- [4] ———, *Whitney forms: A new class of finite elements for three-dimensional computations in electromagnetics*, IEE Proc. A, 135 (1988), pp. 493–500.

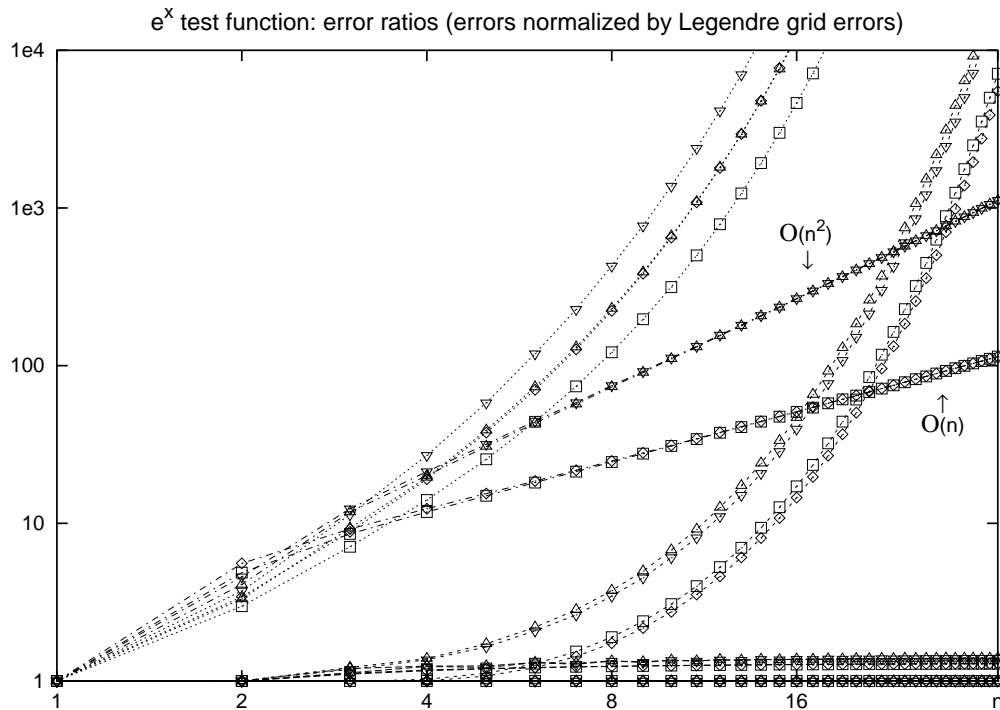


Fig. 20.4: Test function: e^x . MAX and RMS errors normalized by the Legendre grid MAX and RMS errors, as functions of the number n of degrees of freedom, for all grids. See Figure 20.2 for the key. From bottom (smallest errors and ratios) to top (largest errors and ratios), for $n > 27$: Legendre grid (faces at Legendre extrema and endpoints, and nodes at Legendre zeros, which is optimal), optimized Chebyshev grid (faces at Chebyshev extrema and endpoints, and optimal nodes), Chebyshev grid (faces at Chebyshev extrema and endpoints, and nodes at Chebyshev zeros, which is not optimal), optimized uniform grid (cells with lengths $2/n$, and optimal nodes), and uniform grid (cells with lengths $2/n$, and nodes at the center of cells, which is not optimal; the ratios are off the chart for $n > 23$). Comments: The Legendre grid is best, followed closely by the optimized Chebyshev grid. For small n , the optimized grids (Legendre, Chebyshev and uniform) have much smaller errors than the non-optimized ones (Chebyshev and uniform). For large n , the Legendre and optimized Chebyshev grids are much better than the others, and the plain and optimized uniform grids, much worse. (Note however that all grids yield errors smaller than 10^{-45} when $n > 34$, so an error ratio of 10^8 is not damning.) The widening gaps between the errors for plain and optimized grids validate the superconvergence claims. For example, the ratios of the MAX errors for the plain Chebyshev grid and the MAX errors for the optimized Chebyshev grids are $O(n^2)$, and the corresponding RMS error ratios are $O(n)$.

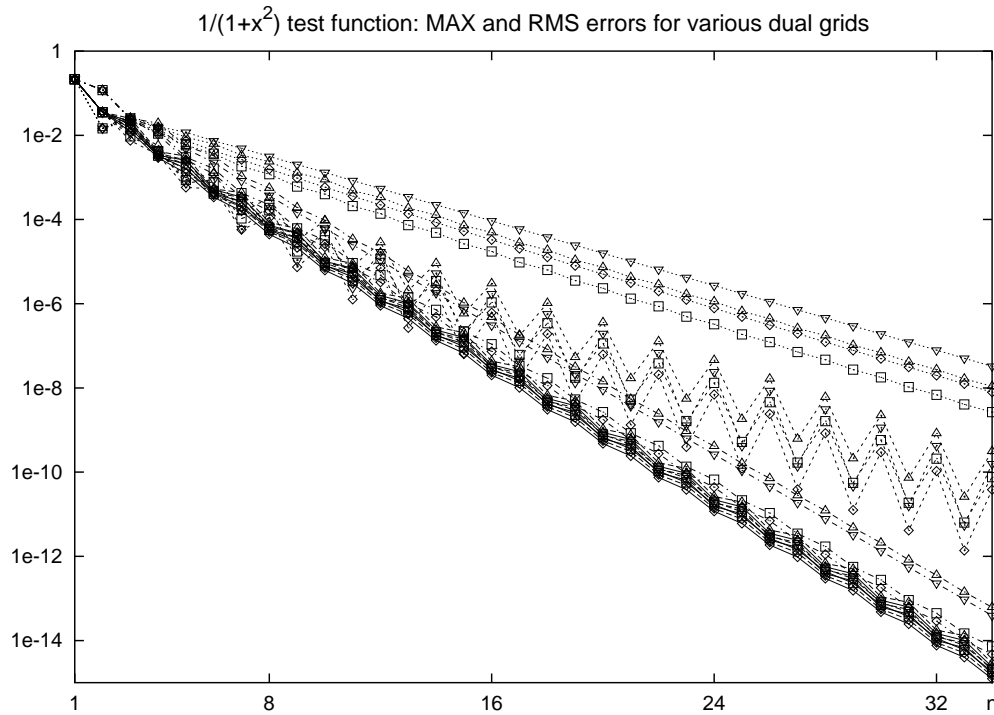


Fig. 20.5: Test function: $1/(1+x^2)$. MAX and RMS errors, as functions of the number n of degrees of freedom, for all grids. See Figure 20.2 for the key, and compare with Figure 20.3. The nodal and average values computed by \star and its inverse converge exponentially for all grids. Comment: The oscillations appear to relate to the presence, when n is odd, of a node at the extremum of $1/(1+x^2)$.

- [5] ———, *Computational electromagnetism*, Academic Press Inc., San Diego, CA, 1998. Variational formulations, complementarity, edge elements.
- [6] ———, *How weak is the “weak solution” in finite element methods?*, IEEE Trans. Magnetics, 34 (1998), pp. 2429–2432.
- [7] ———, *The discrete Hodge operator in electromagnetic wave propagation problems*, in Mathematical and numerical aspects of wave propagation (Santiago de Compostela, 2000), SIAM, Philadelphia, PA, 2000, pp. 753–759.
- [8] ———, *‘Generalized finite differences’ in computational electromagnetics*, in Teixeira [50], pp. 45–64.
- [9] J. P. BOYD, *Chebyshev and Fourier spectral methods*, Dover Publications Inc., Mineola, NY, second ed., 2001.
- [10] F. BREZZI, J. DOUGLAS, JR., R. DURÁN, AND M. FORTIN, *Mixed finite elements for second order elliptic problems in three variables*, Numer. Math., 51 (1987), pp. 237–250.
- [11] F. BREZZI AND M. FORTIN, *Mixed and hybrid finite element methods*, vol. 15 of Springer Series in Computational Mathematics, Springer-Verlag, New York, 1991.
- [12] A. S. CAVARETTA, JR., C. A. MICCHELLI, AND A. SHARMA, *Multivariate interpolation and the Radon transform. II. Some further examples*, in Quantitative approximation (Proc. Internat. Sympos., Bonn, 1979), Academic Press, New York, 1980, pp. 49–62.
- [13] J. A. CHARD AND V. SHAPIRO, *A multivector data structure for differential forms and equations*, Math. Comput. Simulation, 54 (2000), pp. 33–64.

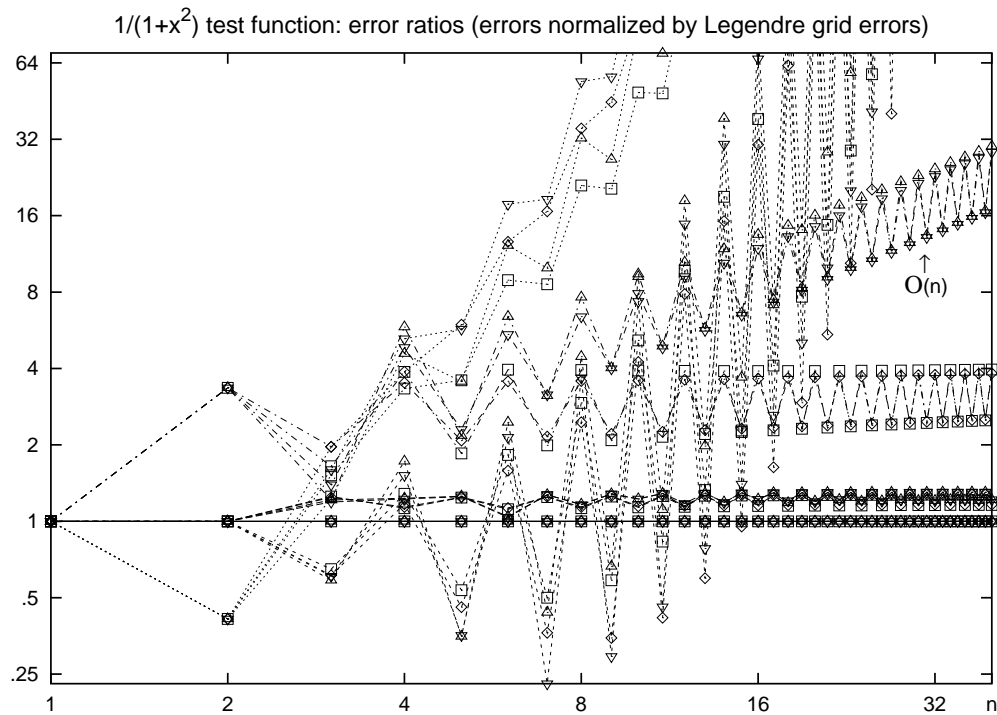


Fig. 20.6: Test function: $1/(1+x^2)$. MAX and RMS errors normalized by the Legendre grid MAX and RMS errors, as functions of the number n of degrees of freedom, for all grids. See Figure 20.2 for the key, and compare with Figure 20.4. For large n , the “ranking” of the grids is the same as for the test function e^x . The only significant changes are that the difference between the plain and optimized Chebyshev grids is not as pronounced as for e^x , and that, for small n , the optimized uniform grid yields the smallest errors when n is odd. Comments: The good performance of the plain and optimized uniform grids for small n can be attributed to the fact that the Jacobi grids have less points near the center of the interval, where the test function varies most rapidly.

- [14] M. CLEMENS, P. THOMA, T. WEILAND, AND U. VAN RIENEN, *Computational electromagnetic-field calculation with the finite-integration method*, *Surv. Math. Ind.*, 8 (1999), pp. 213–232.
- [15] M. CLEMENS AND T. WEILAND, *Discrete electromagnetism with the Finite Integration Technique*, in Teixeira [50], pp. 65–87.
- [16] E. A. COUTSIAS, T. HAGSTROM, AND D. TORRES, *An efficient spectral method for ordinary differential equations with rational function coefficients*, *Math. Comp.*, 65 (1996), pp. 611–635.
- [17] P. J. DAVIS AND P. RABINOWITZ, *Methods of numerical integration*, Computer Science and Applied Mathematics, Academic Press Inc., Orlando, FL, second ed., 1984.
- [18] C. DE BOOR, *A practical guide to splines*, vol. 27 of Applied Mathematical Sciences, Springer-Verlag, New York, 1978.
- [19] A. T. DE HOOP AND I. E. LAGER, *Domain-integrated field approach to static magnetic field computation—application to some two-dimensional configurations*, *IEEE Trans. Magnetics*, 36 (2000), pp. 654–658.
- [20] A. T. DE HOOP, I. E. LAGER, AND P. JORNA, *The space-time integrated model of electromag-*

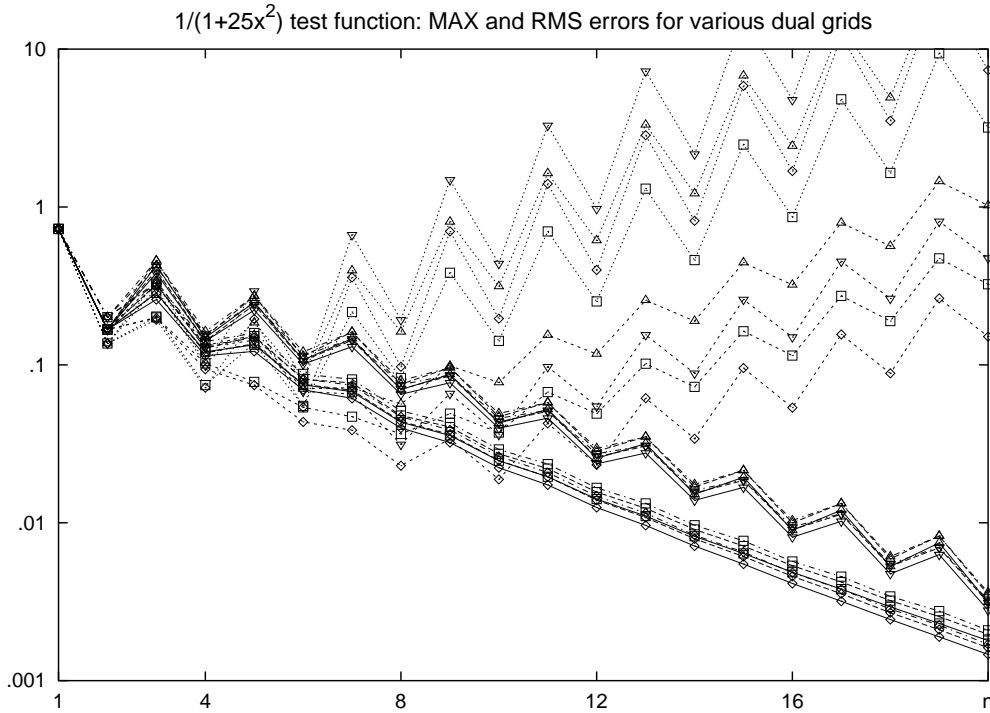


Fig. 20.7: Test function: $1/(1 + 25x^2)$. MAX and RMS errors, as functions of the number n of degrees of freedom, for all grids. See Figure 20.2 for the key, and compare with Figure 20.5. For large n , the “ranking” of the grids is the same as for the test function e^x . The nodal and average values computed by ★ and its inverse converge exponentially for the Legendre and plain and optimized Chebyshev grids, and diverge for the plain and optimized uniform grids.

netic field computation, Electromagnetics, (2002), pp. 371–379.

[21] F.-J. DELVOS, *Periodic area matching interpolation*, in Numerical methods of approximation theory, Vol. 8 (Oberwolfach, 1986), vol. 81 of Internat. Schriftenreihe Numer. Math., Birkhäuser, Basel, 1987, pp. 54–66.

[22] A. A. DEZIN, *Multidimensional analysis and discrete models*, CRC Press, Boca Raton, FL, 1995. Translated from the Russian by Irene Aleksanova.

[23] J. DIEUDONNÉ, *Foundations of modern analysis*, Academic Press, New York, 1969. Enlarged and corrected printing, Pure and Applied Mathematics, Vol. 10-I.

[24] H. ENGELS, *Numerical quadrature and cubature*, Academic Press Inc. [Harcourt Brace Jovanovich Publishers], London, 1980. Computational Mathematics and Applications.

[25] V. GRADINARU AND R. HIPTMAIR, *Whitney elements on pyramids*, Electron. Trans. Numer. Anal., 8 (1999), pp. 154–168 (electronic).

[26] G. HÄMMERLIN AND K.-H. HOFFMANN, *Numerical mathematics*, Undergraduate Texts in Mathematics, Springer-Verlag, New York, 1991. Translated from the German by Larry Schumaker, Readings in Mathematics.

[27] R. HIPTMAIR, *Discrete Hodge operators*, Numer. Math., 90 (2001), pp. 265–289.

[28] ———, *Discrete Hodge-operators: An algebraic perspective*, in Teixeira [50], pp. 247–269.

[29] ———, *High order Whitney forms*, J. Electr. Waves and Appl., 15 (2001), pp. 291–436.

[30] J. M. HYMAN, R. J. KNAPP, AND J. C. SCOVEL, *High order finite volume approximations of differential operators on nonuniform grids*, Phys. D, 60 (1992), pp. 112–138. Experimental

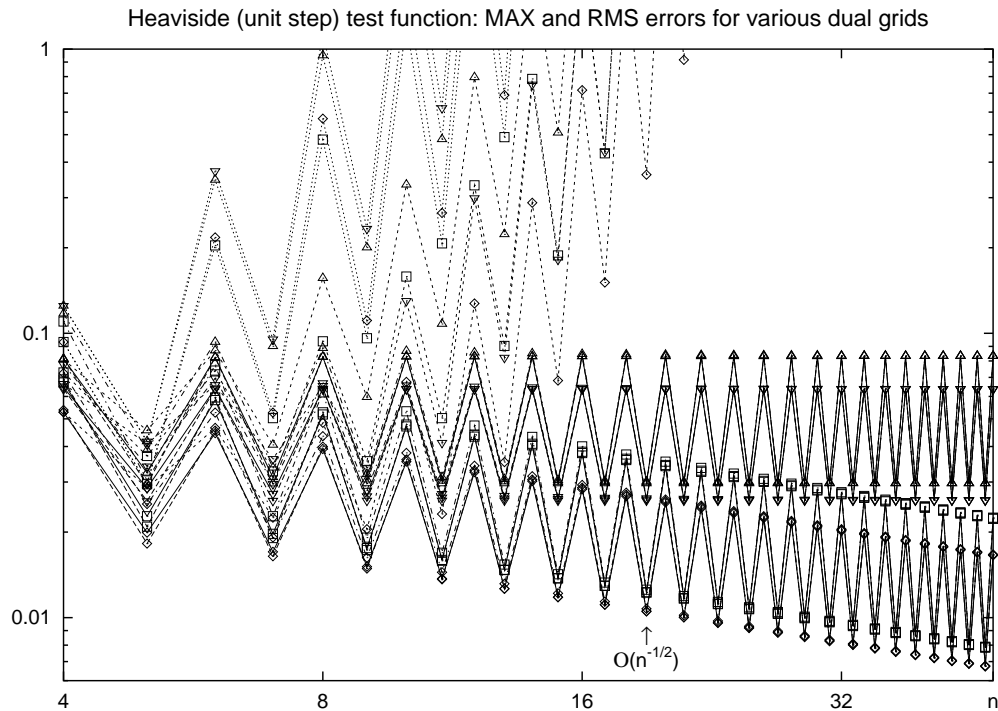


Fig. 20.8: Test function: Heaviside (unit step) function. MAX and RMS errors, as functions of the number n of degrees of freedom, for all grids. See Figure 20.2 for the key. For large n , the MAX and RMS errors for the Legendre and plain and optimized Chebyshev grids are indistinguishable; the RMS errors for these three grids converge at order $1/2$. The good performances of the plain and optimized uniform grids for small n can be attributed to these grids being denser near the jump. The oscillations can be attributed to that, for n odd, every grid has a node at the jump location.

- mathematics: computational issues in nonlinear science (Los Alamos, NM, 1991).
- [31] J. M. HYMAN AND J. C. SCOVEL, *Deriving mimetic difference approximations to differential operators using algebraic topology*, tech. report, Los Alamos National Laboratory, Los Alamos, NM 87545, 1988.
 - [32] J. M. HYMAN AND M. J. SHASHKOV, *Natural discretizations for the divergence, gradient, and curl on logically rectangular grids*, *Comput. Math. Appl.*, 33 (1997), pp. 81–104.
 - [33] J. M. HYMAN AND S. STEINBERG, *Convergence of mimetic discretization for rough grids*. Submitted for publication.
 - [34] R. D. JENKS AND R. S. SUTOR, *AXIOM, the scientific computation system*, Numerical Algorithms Group Ltd., Oxford, 1992. With a foreword by David V. Chudnovsky and Gregory V. Chudnovsky.
 - [35] C. MATTIUSI, *The finite volume, finite element, and finite difference methods as numerical methods for physical field problems*, *Advances in Imaging and Electron Physics*, 113 (2000), pp. 1–146.
 - [36] ———, *A reference discretization strategy for the numerical solution of physical field problems*, *Advances in Imaging and Electron Physics*, 121 (2002), pp. 143–279.
 - [37] R. S. PALMER, *Chain models and finite element analysis: an executable CHAINS formulation of plane stress*, *Comput. Aided Geom. Design*, 12 (1995), pp. 733–770. Grid generation,

- finite elements, and geometric design.
- [38] R. S. PALMER AND V. SHAPIRO, *Chain models of physical behavior for engineering analysis and design*, Research in Engineering Design, 5 (1993), pp. 161–184.
 - [39] N. ROBIDOUX, *A new method of construction of adjoint gradients and divergences on logically rectangular smooth grids*, in Finite Volumes for Complex Applications: Problems and Perspectives, First International Symposium, July 15–18, 1996, Rouen, France, F. Benkaldoun and R. Vilsmeier, eds., Paris, 1996, Editions Hermès, pp. 261–272.
 - [40] ———, *Computer algebra and interpolation: A lesson plan*, Journal of Symbolic Computation, 23 (1997), pp. 551–576.
 - [41] ———, *Numerical Solution of the Steady Diffusion Equation with Discontinuous Coefficients*, PhD thesis, University of New Mexico, Albuquerque, NM, May 2002.
 - [42] W. RUDIN, *Real and complex analysis*, McGraw-Hill Book Co., New York, third ed., 1987.
 - [43] J. W. SCHMIDT, *Beiträge zur konvexen Interpolation, Histopolation und Approximation durch Spline-Funktionen*, Mitt. Math. Ges. Hamburg, 12 (1991), pp. 603–628. Mathematische Wissenschaften gestern und heute. 300 Jahre Mathematische Gesellschaft in Hamburg, Teil 3 (Hamburg, 1990).
 - [44] J. W. SCHMIDT AND W. HESS, *Shape preserving C^2 -spline histopolation*, J. Approx. Theory, 75 (1993), pp. 325–345.
 - [45] I. J. SCHOENBERG, *Splines and histograms*, in Spline functions and approximation theory (Proc. Sympos., Univ. Alberta, Edmonton, Alta., 1972), Birkhäuser, Basel, 1973, pp. 277–327. Internat. Ser. Numer. Math., Vol. 21.
 - [46] H. SPÄTH, *Zur Glättung empirischer Häufigkeitsverteilungen*, Computing (Arch. Elektron. Rechnen), 10 (1972), pp. 353–357.
 - [47] S. STEINBERG, *A discrete calculus with applications to discretizing boundary-value problems*. Preprint. Available from <http://math.unm.edu/~stanly/>, 2002.
 - [48] J. STOER AND R. BULIRSCH, *Introduction to numerical analysis*, vol. 12 of Texts in Applied Mathematics, Springer-Verlag, New York, second ed., 1993. Translated from the German by R. Bartels, W. Gautschi and C. Witzgall.
 - [49] T. TARHASAARI, L. KETTUNEN, AND A. BOSSAVIT, *Some realizations of a discrete Hodge operator: A reinterpretation of finite element techniques*, IEEE Trans. Magn., 35 (1999), pp. 1494–1497.
 - [50] F. L. TEIXEIRA, ed., *Geometric Methods in Computational Electromagnetics, PIER 32*, EMW Publishing, Cambridge, Mass., 2001.
 - [51] F. L. TEIXEIRA AND W. C. CHEW, *Differential forms, metrics, and the reflectionless absorption of electromagnetic waves*, J. Electromagn. Waves Applicat., 13 (1999), pp. 665–686.
 - [52] ———, *Lattice electromagnetic theory from a topological viewpoint*, J. Math. Phys., 40 (1999), pp. 169–187.
 - [53] E. TONTI, *On the geometrical structure of electromagnetism*, in Gravitation, Electromagnetism and Geometrical Structures, G. Ferrarese, ed., Pitagora, Bologna, 1996, pp. 281–308.
 - [54] ———, *Finite formulation of the electromagnetic field*, in Teixeira [50], pp. 1–44.
 - [55] J. H. VERNER. Private communication, February 2003.
 - [56] T. WEILAND, *Time domain electromagnetic field computation with finite difference methods*, Int. J. Num. Modelling, 9 (1996), pp. 295–319.